Palladium-Based Electrocatalysts for Alcohol Oxidation in Half Cells and in Direct Alcohol Fuel Cells

Claudio Bianchini*,† and Pei Kang Shen*,‡

Istituto di Chimica dei Composti OrganoMetallici (ICCOM-CNR), Via Madonna del Piano 10, 50019 Sesto Fiorentino, Italy, and The State Key Laboratory of Optoelectronic Materials and Technologies, School of Physics and Engineering, Sun Yat-Sen University, Guangzhou 510275, P.R. China

Received March 12, 2009

Contents

1. Introduction

Direct alcohol fuel cells (DAFCs) are attracting increasing interest as power sources for portable applications due to some unquestionable advantages over analogous devices fed with hydrogen.[1] Alcohols, such as methanol, ethanol, ethylene glycol, and glycerol, exhibit high volumetric energy density, and their storage and transport are much easier as compared to hydrogen. On the other hand, the oxidation kinetics of any alcohol are much slower and still H_2-fueled *polymer electrolyte fuel cells* (PEMFCs) exhibit superior electrical performance as compared to DAFCs with comparable electroactive surface areas.[2,3] Increasing research efforts are therefore being carried out to design and develop more efficient anode electrocatalysts for DAFCs.

The most common DAFC is the *direct methanol fuel cell* (DMFC), of which there exist also commercial devices with powers spanning from a few watts to 100 W.[4,5] The large majority of DMFCs, either monoplanar cells for laboratory testing or commercial stacks, operate in acidic media with anode catalysts containing Pt and make use of solid electrolytes constituted by proton exchange membranes of the Nafion family.[6] These DMFCs, however, suffer some disadvantages: CO poisoning of the Pt-based catalysts, effective methanol crossover, degradation of the membrane, and corrosion of the carbon materials and cell hardware.[4] As a result, the fuel utilization and the cell voltage are lower than expected and an excess of Pt loading, often alloyed with Ru or Sn, is required for long lasting applications. Overall, these drawbacks, together with the relative toxicity of methanol, are boosting research aimed at using other alcohols as fuels in DAFCs. Indeed, several higher molecular weight alcohols and polyalcohols are featured by high solubility in water, low toxicity, high boiling point, high specific energy, and the capacity of some of them to be renewable. Included in this group are ethanol, ethylene glycol, and glycerol. The former can be massively produced from biomass feedstocks originating from agriculture (first-generation bioethanol), and forestry and urban residues (second-generation bioethanol). Ethylene glycol can be produced by heterogeneous hydrogenation of cellulose, while glycerol is a byproduct of biodiesel production and, as such, is inexpensive and largely available. These alcohols, however, are difficult to oxidize on platinum or platinum alloys. In particular, no known anode catalyst based on platinum has demonstrated the capacity to produce acceptable power densities in either a *direct ethanol fuel cell* (DEFC)[1] or a *direct glycerol fuel cell* (DGFC),[1] unless a partially inorganic solid electrolyte is used at temperatures > 130 °C.[7]

Notable efforts are therefore being carried out to design new catalytic structures for DAFC anodes that do not contain platinum or contain tiny amounts of this rare metal and, most of all, are able to oxidize primary and secondary alcohols with fast kinetics and tolerable deactivation. Within this context, palladium is emerging as an attractive replacement for platinum in DAFCs. Palladium is more abundant in nature and less expensive than platinum,[8] but cost-associated issues

* To whom correspondence should be addressed. C.B.: phone (office), +39 0555225280; fax, +39 0555225203; e-mail, claudio.bianchini@iccom.cnr.it. P.K.S.: phone (office), +86-20-84036736; fax, +86-20-84113369; e-mail, stsspk@mail.sysu.edu.cn.
† Istituto di Chimica dei Composti OrganoMetallici (ICCOM-CNR).
‡ Sun Yat-Sen University.

10.1021/cr9000995 CCC: $71.50
Published on Web 07/17/2009

Claudio Bianchini received his "Laurea" in Chemistry from the University of Florence in 1973. Currently, he is the Director of the Institute of Chemistry of Organometallics of the Italian National Research Council (ICCOM-CNR) in Florence (Italy). He is the author of ca. 430 publications in qualified international journals or specialized books, of 43 patents and relative extensions, and of more than 200 presentations in international chemical meetings. His fields of research include the following: homogeneous and heterogeneous catalysis; electrocatalysts and ionomers for fuel cells and electrolyzers; oligomerization, polymerization, and copolymerization catalysis; hydrogen production and storage; asymmetric synthesis and catalysis; and high-pressure IR and NMR spectroscopy. He is the vice-coordinator and a member of the Executive Committee of the Network of Excellence "Integrated Design of Catalytic Nanomaterials for a Sustainable Production" (IDECAT) and of the European Institute of Catalysis (ERIC). Some of the awards he has received are as follows: 1998 Arthur D. Little Lecturer in Inorganic Chemistry (MIT, USA), 2001 Seaborg Memorial Lecture in Inorganic Chemistry (Berkeley, USA), and 2006 Recipient of the G.ICO Senior Award (Interdivisional group of Organometallic Chemistry of the Italian Chemical Society).

Pei Kang Shen obtained his BSc degree in Electrochemistry at Xiamen University in 1982, and he continuously carried out his research and teaching at the same university for seven years before he became a visiting researcher in the United Kingdom. He received his Ph.D. in Chemistry at Essex University in 1992. From then on he has been working at Essex University, Hong Kong University, the City University of Hong Kong, and the South China University of Technology. Since 2001, he has been the Director and Professor of the Advanced Energy Materials Research Laboratory at the Sun Yat-Sen University (Guangzhou, P. R. China). His research interests include fuel cells and batteries, electrochemistry of nanomaterials and of nanocomposite functional materials, and electrochemical engineering.

are not the main driving force behind the increasing interest in palladium, as it remains a rare noble metal whose introduction for a broad technological use would lead to an irreversible increase in its market price. The real attraction for Pd-based electrocatalysts is originated by the fact that, unlike Pt-based electrocatalysts, they can be highly active for the oxidation of a large variety of substrates *in alkaline environment*, where also non-noble metals are sufficiently stable for electrochemical applications. The dilution of Pd with non-noble metals in a smart catalytic architecture capable of rapidly and stably oxidizing alcohols on anode electrodes is expected to decrease the cost of the *membrane electrode assemblies* (MEAs) so as to boost the commercialization of DAFCs, especially those fed with renewable alcohols.

Besides allowing for the potential use of non-noble metal catalysts at both anode and cathode,[9] the DAFCs operating in alkaline media are attracting increasing industrial interest also due to successful developments in the design and production of anion-exchange membranes (AEMs).[10−21] The drawback of traditional *alkaline fuel cells* (AFCs) to undergo electrolyte carbonation is, in fact, strongly minimized by the use of an anion conductive polymeric membrane, while the advantages of operating in alkaline conditions are manifold and include the following:

- Usability of both noble and non-noble metals to manufacture the electrocatalysts.
- Improved kinetics at both cathode and anode, in particular low anodic overvoltages for alcohol oxidation.
- Alcohol crossover from the anode compartment to the cathode compartment reduced by electro-osmotic drag of hydrate hydroxyl ions.
- Easier water management, as water is formed at the anode side where an aqueous solution already exists, while the electro-osmotic drag transports water away from the cathode, preventing its flooding.
- Reduced risk of corrosion of the materials, including catalysts and carbons.
- Reduced adsorption of spectrator ions that might limit electrocatalysis.

The progress achieved over the last five years in the design of Pd-based electrocatalysts for the oxidation of alcohols, with emphasis on renewable ones, in alkaline media, is reviewed in this article, where particular attention is dedicated to discuss the important roles played by the Pd nanostructure and by the support material in governing the kinetics and selectivity of the oxidation process as well as the catalyst lifetime.

2. Preparation and Characterization of Pd-Based Electrocatalysts

The most common synthetic routes to Pd-based catalysts with proven activity for the oxidation of alcohols in either half cells or DAFCs are reviewed in the following sections, together with their chemical−physical characterization.

Current methods for the preparation of Pd-based electrocatalysts, which are effective for alcohol oxidation, are manifold and include the electroless reduction and the hydrothermal treatment of high-valent Pd compounds; the synthesis of Pd colloids, sol−gels, microemulsions, or reversed micelles and their deposition onto appropriate electron-conductive supports; the electrodeposition of Pd films, wires, and nanoparticles; and transmetalation reactions where high-valent Pd compounds are reacted with less noble metal phases. Depending on the type and number of the metal precursors or on the specific synthetic protocol, alloys or composite materials can also be obtained.

In general, the catalysts are isolated either as supported metal particles or as Pd thin films, with the best performance for alcohol oxidation exhibited by nanosized Pd electrocatalysts. The nanosize is often a necessary requirement, yet it

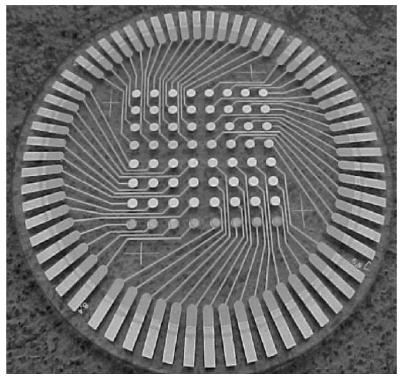

Figure 1. 64-Element addressable electrode array used as support for the synthesis of chemically diverse electrocatalyst libraries. Image is from ref 22.

is not *per se* sufficient to ensure high catalytic activity or to combine high activity with durability and stability. As will be shown in forthcoming pages, there are many other factors to take into account for the design of an effective and stable Pd electrocatalyst for alcohol oxidation; in particular, of crucial importance are the morphology, shape, and dispersion of the metal particles and the nature of the support material. This is generally constituted by a carbon black (CB), yet an increasing role is being played by different nanostructured carbon materials (tubes, wires, fibers, etc.) as well as composites where a carbon black or a carbonized material is combined with other metals or metal oxides, which may also promote or control the alcohol oxidation on Pd. Indeed, in addition to CBs, such as Vulcan XC-72 or Ketjen black, alone or in combination with either nanocrystalline metal oxides or metal carbides, a huge variety of carbonaceous materials have been used to support and stabilize Pd nanoparticles: carbon microspheres, coinlike hollow carbons, ultrahigh-surface hollow carbon spheres, carbon nanotubes and nanofibers, carbonized porous anodic alumina, and carbonized TiO_2 nanotubes.

Physical methods for Pd electrocatalysts characterization include high resolution electron microscopy (HRTEM), extended X-ray absorption fine structure spectroscopy (EXAFS), energy dispersive spectroscopy (EDS), inductively coupled plasma atomic emission spectroscopy (ICP-AES), near edge X-ray absorption spectroscopy (XANES), X-ray powder diffraction (XRPD), and infrared and Raman spectroscopy (IR, RS).

Electrochemical characterization methods include cyclic voltammetry (CV), chronopotentiometry, chronoamperometry, AC impedance spectroscopy, *in situ* spectroelectrochemistry, and electrochemical scanning tunneling microscope. Fast electrocatalyst screening has been achieved by scanning electrochemical microscopy. Strasser et al. have described a device for the high throughput electrochemical screening constituted by an array of 64 individually addressable, circular electrode pads (0.02 cm^2 each), fabricated using lithographic techniques on an insulating 3 in. quartz wafer (Figure 1).[22] The electrode pads provide ohmic contacts with the catalytic electrode materials to be deposited thereon, interfacing the materials library and a multichannel potentiostat/galvanostat.

2.1. Supported Pd Electrocatalysts

The main requirements of a suitable support for a FC electrocatalyst are high surface area, good electrical and thermal conductivity, suitable porosity to allow for a good reactant flow, and high stability in the FC environment. CBs meet most of these characteristics, yet they exhibit low stability to corrosion, especially in acidic media at high potential (cathode side) and high temperatures (>90 °C). On the other hand, the large availability and the low cost make CBs, and in particular Vulcan-type materials, still the most diffuse supports for low-temperature FC electrocatalysts. Moreover, CBs can be easily activated to increase the number of the anchoring centers that can favor the formation of highly dispersed and strongly bound metal phases.

For the sake of clarity, all the Vulcan-supported Pd catalysts described in this article will be referred to as Pd/C.

The large majority of carbon-supported electrocatalysts are prepared by reduction of physi- and chemisorbed metal salts or metal complexes with a chemical reductant ($NaBH_4$, ethylene glycol, hydrazine, tannic acid, formic acid, formaldehyde, hydrogen gas) that may also act as templating agent to favor the formation of nanosized metal particles.[23−25] The Pd particles obtained by electroless procedures are generally well dispersed and crystalline, with dimensions in the range from 3 to 25 nm, and the X-ray power diffraction (XRPD) patterns show face-centered cubic (fcc) lattice structures with diffraction peaks at the Bragg angles of 40.10°, 46.40°, and 68.08°, corresponding to the (111), (200), and (220) facets of a palladium crystal. A shift of the 2θ values may be indicative of the formation of Pd alloys with other metals.

As an alternative to the reduction of metal salts or compounds adsorbed on conductive materials, surfactant-stabilized colloidal Pd can be independently prepared *via* the Bönneman method and later mixed with carbon black.[26] Binary PtPd/C and ternary PtPdBi/C catalysts have been prepared by the water-in-oil microemulsion method, involving the reduction of different microemulsions of metal salts, successively added to a conductive carbon.[27] Huang has prepared Pd/C electrocatalyst using $(WO_3)_n \cdot xH_2O$ as *in situ* colloidal source, obtaining metal particles with an average size of 3.3 nm and a narrow size distribution.[28]

The intermittent microwave heating (IMH) is an effective and fast method for the synthesis of a variety of nanostructured metal electrocatalysts recently described by Shen.[29,30] As a general procedure, the catalyst precursor, the supporting materials, and the reducing agent are mixed in water and the mixture is heated in a program-controlled microwave oven. The resulting electrocatalyst powders are generally small (3−10 nm) and can be uniformly dispersed in water and alcohols to give stable suspensions. As will be shown in forthcoming pages, many Pd-based catalysts prepared by the IMH method provide excellent performance for the oxidation of various alcohols.

A very elegant procedure to synthesize C-supported submonolayer Pd-decorated Au nanoparticles has been recently reported by Zhao and successfully used for the electrooxidation of ethanol in alkaline media.[31] The Pd@Au/C catalyst was obtained through a stepwise route involving the synthesis of Au seeds with a mean size of 4.0 nm, followed by chemically epitaxial growth of Pd on the Au surface.

Another class of carbon supports for FC electrocatalysts is represented by carbon nanotubes (CNTs). The high crystallinity of CNTs makes these materials highly conductive, while the high surface area and the great number of mesopores can lead to high metal dispersion and a good reactant flux in the tubular graphite structure. It has been

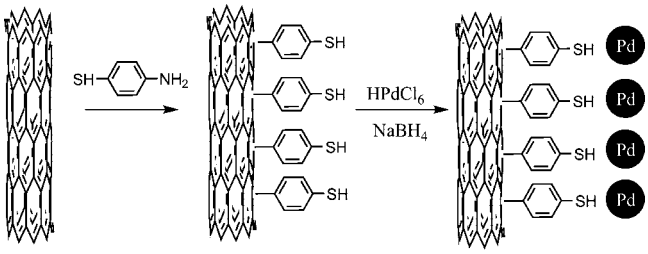

Figure 2. Self-assembly synthesis of Pd nanoparticles on functionalized MWCNTs. Image is from ref 38.

established that the increase in the graphitization degree of the carbon material increases the π sites which can act as anchoring centers for the metal nanoparticles. As a result, the metal−support interactions and the resistance of the support to oxidation are improved, while the metal sintering is disfavored.[32−34]

Multiwalled carbon nanotubes (MWCNTs) and their functionalized derivatives are already a widespread support material for FC electrocatalysts. Several ways to pretreat MWCNTs for use as support for metal electrocatalysts have been recently reported in the literature.[35−37] Sun has developed a simple approach to prepare sulfonated MWCNTs, leading to effective Pd catalysts for methanol oxidation,[35] while Hu has treated MWCNTs with hydrofluoric acid, obtaining a material with enlarged micropores that is capable of anchoring the Pd nanoparticles so effectively that neither agglomeration nor detachment are observed during ethanol oxidation.[37] The self-assembly of Pd nanoparticles on MWCNTs functionalized with mercaptobenzene moieties has been recently developed by Li and co-workers.[38] The elegant synthetic procedure to these materials, later tested for the oxidation of formaldehyde in alkaline solution, is shown in Figure 2.

Yen has introduced the use of the chemical fluid deposition technique to prepare MWCNT-supported bimetallic nanoparticles that are effective for methanol oxidation,[37] while Singh and Anindita have prepared PdNi bimetallic electrocatalysts, with different Pd to Ni ratios, for ethanol oxidation in alkaline solution, proving that the addition of MWCNTs (1−5%) greatly increases the activity.[40]

Shen et al. have compared the catalytic activity for ethanol oxidation of Pd nanoparticles supported on MWCNTs, Vulcan XC-72, and active carbon fibers (ACFs) prepared by the IMH technique.[24] Figure 3 shows the corresponding TEM images.

A further evidence of the ability of MWCNTs to contribute to the formation of excellent Pd electrocatalysts for alcohol oxidation has been reported by Bianchini and Serp et al.[41] These authors have synthesized a nanostructured Pd/MWCNT catalyst by treatment of MWCNT-adsorbed $Pd_2(dba)_3$ with H_2 (dba = benzylideneacetone) (Figure 4) and have evaluated its performance for the oxidation of methanol, ethanol, and glycerol in 2 mol dm^{-3} KOH solutions. The electrocatalyst exhibits high activity for the oxidation reaction of all alcohols even at metal loadings as low as 17−20 μg cm^{-2} (*vide infra*).

Other materials with nanotube morphology have been successfully employed to prepare Pd-based electrocatalysts for DAFCs. Li et al. have described the synthesis of Pd particles supported on a large variety of nanotubes, including MWCNTs,[35] TiO_2 nanotubes,[42] vanadium oxide nanotubes,[43] and β-MnO_2 nanotubes,[44] and used them as electrocatalysts for alcohol oxidation. A typical FESEM micrograph of the β-MnO_2 nanotubes and a TEM image of the Pd particles supported on β-MnO_2 nanotubes are shown in Figure 5. The Pd nanoparticles are homogeneously dispersed and well separated from one another on the surfaces of the β-MnO_2 nanotubes.

Some papers have also appeared reporting on the use of carbon microspheres (CMSs),[45] coinlike hollow carbons (CHCs),[46] and ultrahigh-surface hollow carbon spheres (HCSs)[47] as support material for Pd electrocatalysts. As will be shown in forthcoming pages, the application of some of these electrocatalysts in DAFCs provides quite interesting results.

The replacement of CBs by CMSs has been found to induce significant changes in the catalytic layer structure of the FC electrodes. Indeed, the primary carbon nanoparticles, being tridimensionally linked through covalent bonds, can form a macroscopic monolithic structure with high porosity and good electronic conductivity.[45] This particular structure of the carbon microspheres prevents the formation of small or even closed pores in the electrode catalytic layer, while the high surface area and the large number of mesopores of the ordered mesoporous carbons and carbon gels allow for the obtainment of high metal dispersion and good reactant flux. Accordingly, catalysts supported on CMSs generally show higher catalytic activity as compared to the same metal phases supported on a traditional, mesoporous CB.

Tungsten carbide (WC) nanocrystals, prepared by the IMH method, have been recently employed as supports for Pd nanoparticles.[48−51] The resulting Pd-WC/C catalysts provide better results for the oxidation of ethanol in alkaline media than Pd/C, which has been suggested to be due to the higher electrochemically active surface area (EASA) of Pd-WC/C as well as a synergistic effect between the Pd particles and the WC support.[49]

The combination of nanostructured Pd with other late transition metals or metal oxides has recently originated a distinctive class of electrocatalysts for DAFC applications. The first report dealing with the synthesis and electrochemical characterization of Pd/C electrocatalysts promoted by nanocrystalline late transition metal oxides appeared in 2006 by Shen and Xu.[23] These authors demonstrated that the electroless reduction of $PdCl_2$ adsorbed onto oxide/C materials

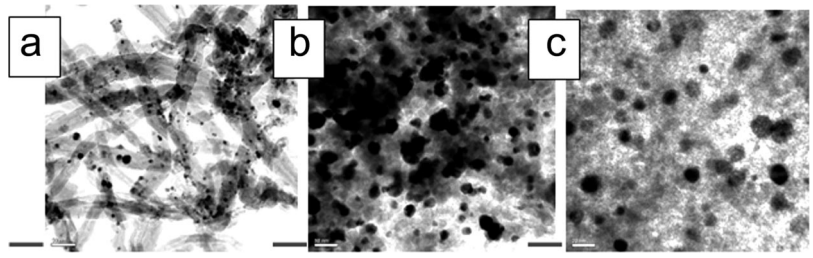

Figure 3. TEM images of (a) Pd/MWCNTs, (b) Pd/C, and (c) Pd/ACF prepared by the IMH method. Images are from ref 24.

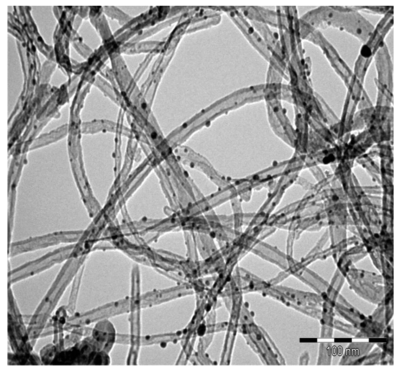

Figure 4. TEM micrograph of Pd/MWCNT (scale bar: 100 nm). Image is from ref 41.

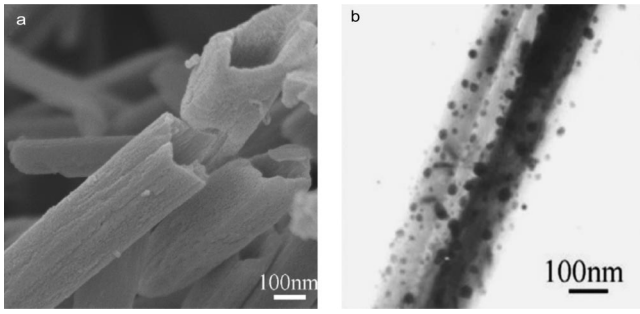

Figure 5. (a) FESEM micrograph of β-MnO_2 nanotubes and (b) TEM image of Pd/β-MnO_2 nanotubes. Images are from ref 44.

(oxide = CeO_2, Co_3O_4, Mn_3O_4, NiO) yields electrocatalysts for alcohol oxidation exhibiting much higher catalytic activity (in terms of onset oxidation potential and peak current density) and electrochemical stability than those of any Pd/C or Pt/C electrocatalyst under comparable experimental conditions.[25,52−54] Figure 6 shows the XRPD patterns of these materials and TEM images of Pd-NiO/C, Pd-Co_3O_4/C, and Pd-Mn_3O_4/C.[52]

The spontaneous deposition (SD) of noble metals onto less noble metal particles or metal surfaces is emerging as a viable technique for creating new catalyst architectures as well as allowing one to introduce single noble metal sites over the surface of a non-noble metal phase.[55−58] Some authors refer to the SD technique as a surface replacement reaction (SRR).[59] A schematic representation of the spontaneous deposition of a high-valent metal *via* redox transmetalation is shown in Figure 7 for a hypothetical non-noble metal phase supported on a conductive material.

Some applications of the SD technique to the preparation of Pd-based electrocatalysts have been recently reported; among these, there are also examples of active anode catalysts for DAFCs.[58,60] Their preparation commonly proceeds by simply stirring a water solution of either a Pd^{II} or Pd^{IV} salt in the presence of an appropriate electropositive metal phase. For example, stirring a water solution of K_2PdCl_4 in the presence of carbon supported Ni-Zn and Ni-Zn-P alloys gives the highly efficient electrocatalysts Pd-(Ni-Zn)/C and Pd-(Ni-Zn-P)/C.[58,60] The characterization of the latter materials by HRTEM, EXAFS, XPRD, and XANES has unambiguously shown their surface to contain very small (0.5−1 nm), highly dispersed, and crystalline Pd and Ni clusters, as bimetallic aggregates, Ni−O, as well as single Pd sites, likely stabilized by the interaction with oxygen atoms from nickel oxide.[58]

As a variation of the SD technique, CNT-supported PtPd hollow nanospheres have been recently obtained by a replacement redox reaction between sacrificial cobalt nanoparticles and $PtCl_6^{2-}$ and Pd^{2+} ions.[61] No information is yet available on the ability of these electrocatalysts to electrochemically oxidize alcohols, as they were exclusively tested for formic acid oxidation.

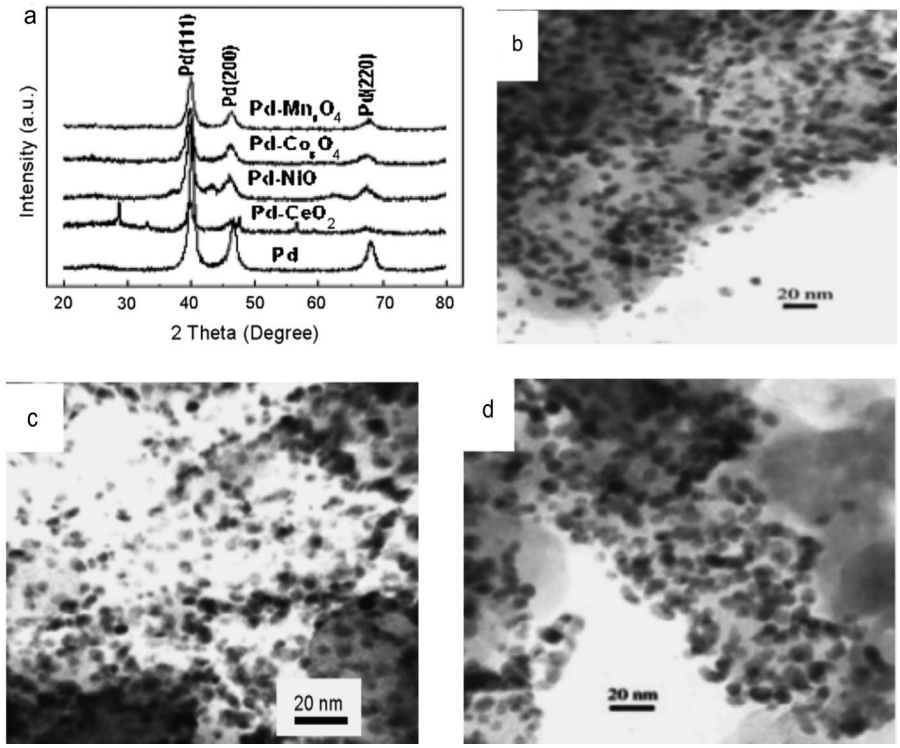

Figure 6. (a) XRD patterns of Pd/C, Pd-CeO_2 (1:1, w:w)/C, Pd-NiO (1:1, w:w)/C, Pd-Co_3O_4 (1:1, w:w)/C, and Pd-Mn_3O_4 (1:1, w:w)/C; (b) TEM image of Pd-NiO (4:1, w:w)/C; (c) TEM image of Pd-Co_3O_4 (4:1, w:w)/C; (d) TEM image of Pd-Mn_3O_4 (4:1, w:w)/C. Images are from ref 52.

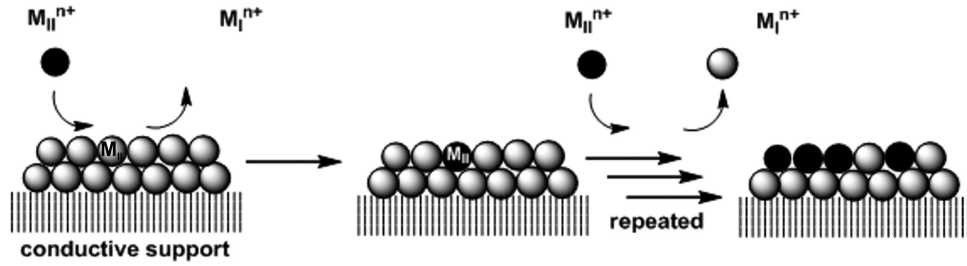

Figure 7. Schematic $metal_{II}$ deposition onto $metal_I$ particles via redox transmetalation.

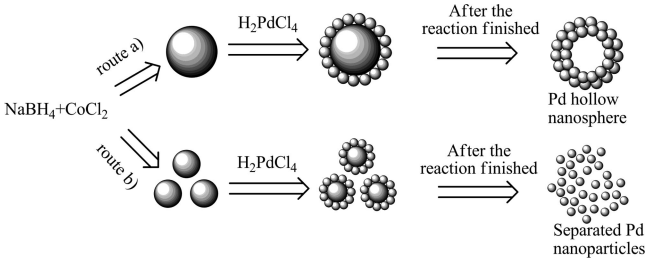

Figure 8. Formation mechanisms of Pd hollow nanospheres and nanoparticles: (route a) Pd hollow nanosphere; (route b) separated Pd nanoparticles in adjusted condition. Image is from ref 59.

Ge et al. have synthesized nanosized carbon-supported Pd electrocatalysts through the SRR illustrated in Figure 8 and have also shown that the particle morphology is greatly influenced by the synthesis conditions: hollow nanospheres were formed at pH = 9, while highly dispersed carbon-supported nanoparticles were obtained at pH 10.[59]

Zheng has reported the preparation of PdPt electrocatalysts for ethanol oxidation by the spontaneous replacement of Pt on Pd film.[62]

2.2. Unsupported Pd Electrocatalysts

Although essentially used for laboratory tests in half cells, a number of unsupported Pd electrocatalysts for alcohol oxidation have been recently reported.

Electrochemical methods involve either the electrodeposition of one metal at a time, eventually followed by the electrodeposition of other metals, or the contemporaneous electrodeposition of two or more metals.

A wide compositional range of NiPd alloys for use as anode catalysts in alkaline DMFCs has been prepared by electrodeposition onto titanium discs using a $PdCl_2$/$NiSO_4 \cdot 7H_2O$ bath.[63] The structural characterization of these electrocatalysts in their as-plated condition is consistent with the formation of a nanocrystalline, single-phase, face centered cubic alloy.

Cyclic potential sweep techniques have been used to prepare Pd thin films on polycrystalline Pt or Au substrates.[64]

The preparation of nanosized Pd arrays and nanowire arrays may proceed by different routes, some of which are highly sophisticated, such as that reported by Safavi which involves the plain electrodeposition from a $PdCl_2$ solution onto a carbon ionic liquid electrode (CILE) using octylpyridinum hexafluorophosphate as a binder.[65]

Highly ordered Pd and PdPt nanowire arrays (PdPt NWAs) have been prepared by template-electrodeposition.[66−68] Figure 9 shows the typical SEM micrographs of Pd NWAs and Pd/Pt core−shell NWAs. The PdPt NWA electrode is featured by a very high EASA and has been found to be much more active than PtRu/C for the methanol oxidation in acidic media. A synergistic effect of the two metals seems to be operative, as Pd electrocatalysts are active for alcohol oxidation exclusively in alkaline media.[68]

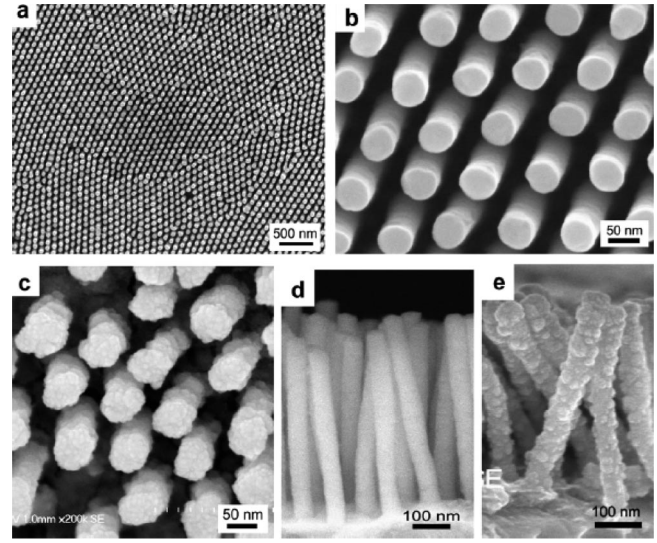

Figure 9. SEM micrographs of (a) and (b) Pd NWAs, (c) Pd/Pt core−shell NWAs, (d) cross-section of Pd NWAs, and (e) cross-section of Pd/Pt core−shell NWAs. Images are from ref 68.

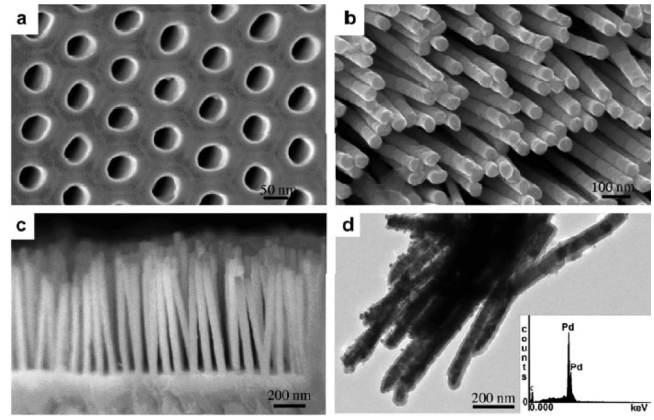

Figure 10. Typical SEM images of (a) AAO template, (b) Pd nanowire array, and (c) cross-section of the Pd nanowire array, and (d) TEM image and EDX (inset) of Pd nanowire array. Images are from ref 67.

Figure 10 shows the morphology of the NWAs, prepared by pulse electrodeposition using a porous aluminum oxide as templating agent.[66,67] These materials exhibit excellent catalytic activity for the oxidation of ethanol,[66] methanol, and isopropanol.[67]

3. Pd-Based Electrocatalysts for Alcohol Oxidation in Alkaline Media

At both the academic and industrial levels, the recent development of efficient and stable anion-exchange mem-

Table 1. Representative Pd-Based Electrocatalysts for Alcohol Oxidation in Alkaline Media

metal	oxide/support	alcohol/strong base coreagent	ref
Pd NWA		ethanol/KOH	66
		methanol, isopropanol/KOH	67
		methanol/KOH	68
Pd	C	ethylene glycol/NaOH	26
	CMSs	methanol, ethanol/KOH	45
	coinlike C	ethanol, methanol, glycerol, EG/KOH	46
	HCSs	methanol/KOH	47
	C, ACF	ethanol/KOH	24
	MWCNT	methanol, ethanol, glycerol	41
	C	2-propanol/KOH	75
Pd	MWCNT	ethanol/KOH	24
	s-MWCNT	methanol/KOH	35
	MWCNT	ethanol/KOH	37
	MWCNT	ethanol/KOH	40
	MWCNT	methanol, ethanol, glycerol/KOH	41
Pd-oxide	TiO_2/C	methanol/H_2SO_4	42
	TiO_2/C	ethanol/KOH	74
	VO_x/C	methanol/NaOH	43
	β-MnO_2	methanol/NaOH	44
	CeO_2/C, Co_3O_4/C, Mn_3O_4/C, NiO/C	methanol, ethanol, EG, glycerol/KOH	25
	CeO_2/C, NiO/C, Co_3O_4/C, Mn_3O_4/C	methanol, ethanol, EG, glycerol/KOH	52
	CeO_2/C, NiO/C	ethanol/KOH	53
	NiO/C	ethanol/KOH	54
	In_2O_3/C	ethanol/KOH	72
	carbonized porous anodic alumina	ethanol/KOH	54
		ethanol/NaOH	72
		methanol, ethanol, EG, glycerol/KOH	73
Pd/WC		ethanol/KOH	49
	WC/CNT	methanol, ethanol, EG/KOH	51
	WC/CNT	ethanol/KOH	55
PdPt		ethanol/KOH	62
	MWCNT	methanol/H_2SO_4	39
PdNi	C	methanol/KOH	63
		ethanol/KOH	40
PdAu	C	methanol/KOH	64
	C	2-propanol, methanol/KOH	77
	C	ethanol/KOH	30
	WC	ethanol/KOH	48
PdRu		ethanol/KOH	82
Pd(Ni-Zn)/C	C	ethanol, methanol, glycerol/KOH	58
Pd(Ni-Zn-P)/C	C		

branes (AEMs) constitutes the main reason for the increasing interest in Pd-based electrocatalysts. The difficult access to AEMs and the relatively easy supply of cation-exchange membranes, especially the commercial Nafion materials, has discouraged, for a long time, chemists from studying electrocatalysts based on metals, such as Pd, that are inactive in acidic media. Pd electrocatalysts are, in fact, active for alcohol and hydrogen oxidation exclusively in alkaline media (*vide infra*). This characteristic is not valid for the oxygen reduction reaction (cathode process in DAFCs), for which Pd-based catalysts are active in both acidic and alkaline media.[9]

At present, there are AEMs that are competitive with Nafion membranes in terms of thermal and chemical stability as well as cost per surface unit, but cation-exchange membranes are still superior in terms of ion conductivity. Nevertheless, in forthcoming pages of this review it will be shown that AEM-DAFCs equipped with Pd-based electrocatalysts at the anode can exhibit power densities as high as 200 mW cm^{-2} at relatively high temperatures ($\leq$80 °C) with several important alcohols such as ethanol and glycerol.

Half cell studies of electrodes containing Pd electrocatalysts for alcohol oxidation constitute the subject of the next section. Such studies are actually propaedeutic to the application of any anode electrode in a DAFC, as only CV, chronopotentiometric, chronoamperometric, AC impedance, and related experiments can provide the necessary information (onset and peak oxidation potentials, current density, stability, selectivity of oxidation, fuel diffusion, resistance, etc.) to develop an effective MEA. A following section will deal with all known AEM-DAFCs that make use of a Pd-based anode electrocatalyst: their number is rapidly increasing together with their capacity to provide high power densities.

Before proceeding with this schedule, it is worth mentioning a point of great importance for understanding and rationalizing the electrochemical performance of the Pd-based anodes: all known Pd-based electrocatalysts are unable to promote selectively the complete oxidation of alcohols to CO_2 in alkaline media (*vide infra*). In particular, ethanol and other primary alcohols are almost exclusively oxidized to the corresponding carboxylic acid, isolated as alkali metal carboxylates, while polyalcohols may undergo C−C bond scission with formation of carbonate, yet this is invariably a minor reaction path as compared to the partial oxidation to carboxylate.

3.1. Half Cell Performance

Table 1 summarizes all the relevant alcohol oxidation reactions on Pd electrodes investigated in half cells. Methanol and ethanol are the most studied substrates, but several data are also available for 1-propanol, 2-propanol, ethylene glycol, and glycerol.

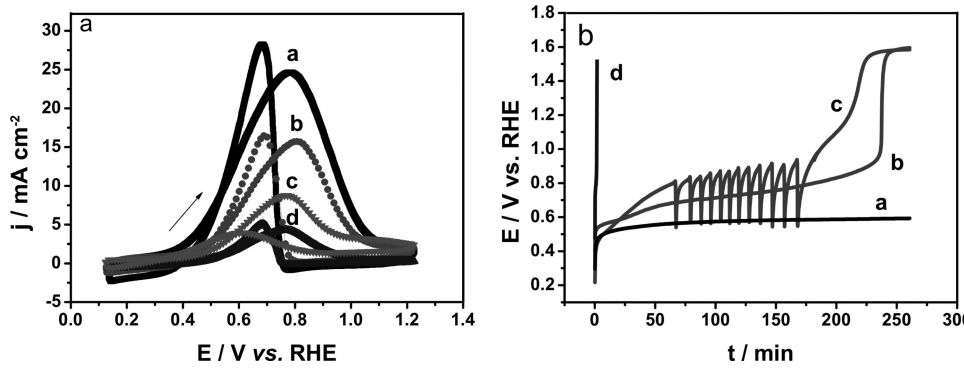

Figure 11. (a) Cyclic voltammograms of different Pd-based electrodes and Pt/C in 1.0 mol dm^{-3} KOH solution containing 1.0 mol dm^{-3} ethanol at a sweep rate of 50 mV s^{-1} at room temperature and a Pd loading of 200 μg cm^{-2}: (a) Pd/MWCNT; (b) Pd/C; (c) Pt/C; (d) Pd/ACF. (b) Chronopotentiometric curves of ethanol oxidation on (a) Pd/MWCNT, (b) Pd/C, (c) Pt/C, and (d) Pd/ACF at 1.0 mA cm^{-2} in 1.0 mol dm^{-3} ethanol + 1.0 mol dm^{-3} KOH solution. Images are from ref 24.

It has been unambiguously established that both the type of the support material and the copresence of other metals or metal oxides can remarkably affect the catalytic performance of Pd catalysts in terms of activity and electrochemical stability. For this reason, the half cell studies have been reviewed according to the nature of the support material. Distinct classes are also reported for catalytic materials where Pd is combined with other noble or non-noble metals.

3.1.1. Pd Electrocatalysts Supported on Carbon Blacks or Other Carbon Materials

The largest number of half cell studies is concerned with nanostructured Pd, alone or alloyed with other metals, supported on carbon materials, spanning from carbon blacks such as C, CMSs, CHCs, HCSs, CNTs, and nanofibers (NFs).

The effect of the carbon support on the activity of nanostructured Pd catalysts for ethanol oxidation has been systematically investigated by Shen and co-workers using $PdCl_2$ as metal precursor and various reducing agents. A number of supports have been considered, including Vulcan XC-72,[24] MWCNTs,[24] ACFs,[24] CMSs,[45] and HCSs.[47] The cyclic voltammograms (CVs) relative to the ethanol oxidation on Pd nanoparticles supported on the first three materials are reported in Figure 11, which also shows the CV of a Pt/C electrode for comparative purposes (trace c). Under comparable experimental conditions (200 μg cm^{-2} Pd), the Pd/MWCNT catalyst is more active than Pd/ACF or Pd/C as well as more electrochemically stable, as shown by chronopotentiometric tests (Figure 11b). Consistent with the higher catalytic activity of Pd/MWCNT, its Nyquist plot shows a lower reaction resistance as compared to Pd/ACF and Pd/C.[24] The smaller size and higher dispersion of the Pd nanoparticles in Pd/MWCNT have been claimed as the factors accounting for the higher catalytic activity of this catalyst as compared to Pd/ACF and Pd/C.

It is worth noticing that, under comparable experimental conditions, not only is the Pt/C electrode much less active, in terms of both the onset potential of ethanol oxidation and the peak current density, but it is also less stable, showing extensive potential oscillation as well as faster attainment of the oxygen-discharge overpotential (Figure 11).

Bianchini, Serp, and co-workers have evaluated the performance of Pd/MWCNT for the oxidation of methanol, ethanol, and glycerol in 2.0 mol dm^{-3} KOH solutions.[41] This catalyst exhibits high activity for the oxidation reaction of all alcohols even at metal loadings as low as 17−20 μg cm^{-2}. In the half cell, glycerol provides the highest peak current density (54 mA cm^{-2}), while ethanol shows the lowest onset potential (+0.27 V vs RHE) (Figure 12). Notably, the Pd/MWCNT electrode is electrochemically stable only for the oxidation of ethanol, while the oxidation reactions of methanol and glycerol are featured by a fast increase of the overpotential.[41]

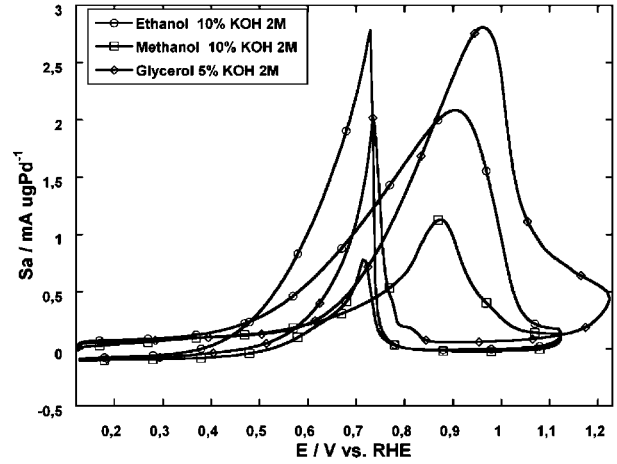

Figure 12. Cyclic voltammograms of methanol, ethanol, and glycerol oxidation on a Pd/MWCNT electrode in 2.0 mol dm^{-3} KOH: Pd loading, 17 μg cm^{-2}; scan rate, 50 mV s^{-1}. Image is from ref 41.

The degradation of the Pd/MWCNT electrode during methanol and glycerol oxidation has been ascribed to the formation of adsorbed CO.[1b,c,9,41] Indeed, while ethanol is selectively oxidized to acetic acid, transformed into acetate ion in the alkaline environment of the reaction, methanol and glycerol give carbonate via CO intermediate.[41] In particular, methanol is fully oxidized to carbonate, while glycerol gives C_3 hydroxy carboxylates and bicarboxylates, but also oxalate, formate, and carbonate *via* C−C bond breaking reactions (*vide infra*). The larger polarization of the Pd/MWCNT electrode during glycerol oxidation as compared to methanol oxidation has been attributed to the formation of strong interactions between the electrode surface, rich in −COOH groups,[69] and the products of the partial oxidation of glycerol, which include hydroxyacids, such as glycolic and glyceric acids, and keto acids, such as tartronic acid.[41,70,71]

It has also been observed that the diffusion of MeOH across the MWCNT support is much faster than the diffusion of ethanol and glycerol, whose oxidation reactions are diffusion-controlled only at low scan rates (<350 mV s^{-1}

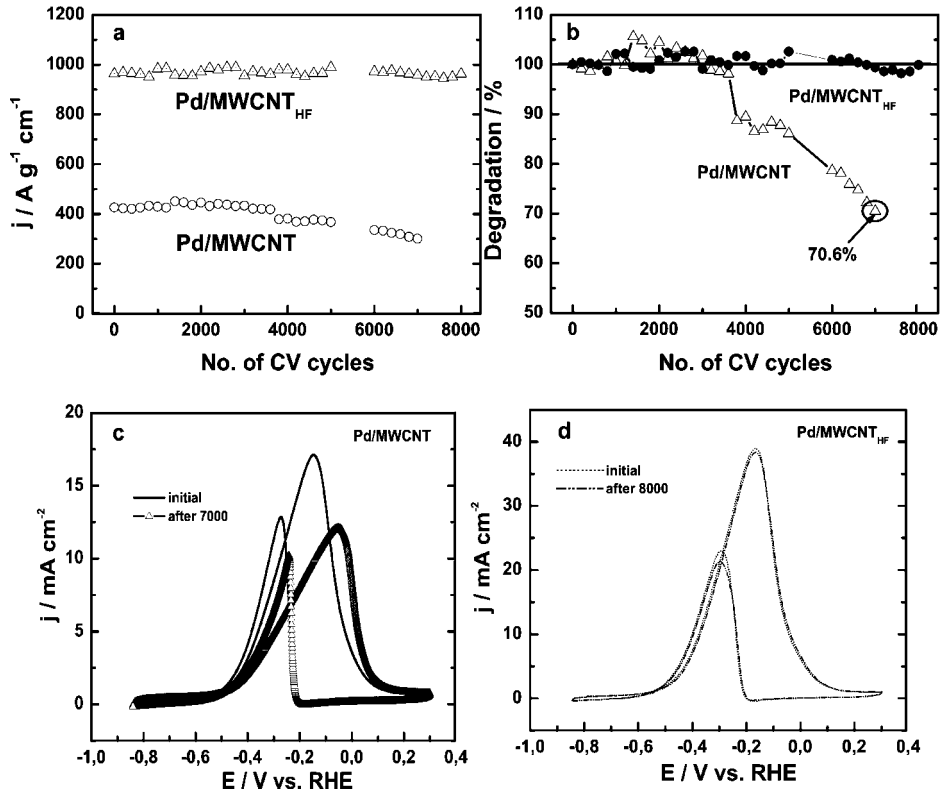

Figure 13. (a) Relationship between mass activity and the CV cycle numbers for ethanol oxidation on Pd/MWCNT and Pd/MWCNT$_{HF}$. (b) Comparison of the degradation as a function of the cycles for the two electrocatalysts. (c) 1st and 7000th cyclic voltammograms of ethanol oxidation on Pd/MWCNT. (d) 1st and 8000th cyclic voltammograms of ethanol oxidation on Pd/MWCNT$_{HF}$. All experiments were performed in 1.0 mol dm^{-3} KOH/1.0 mol dm^{-3} ethanol solution at 303 K. Scan rate: 50 mV s^{-1}. Images are from ref 37.

for ethanol; < 50 mV s^{-1} for glycerol).[41] At higher scan rates, the oxidation kinetics of ethanol and glycerol seem to be controlled by other factors, such as the low density of the catalytic centers and the difficult product desorption. As an indirect confirmation of the ability of the carbon support to control the substrate diffusion, the oxidation of methanol on an electrode catalyzed by Pd/C (same metal loading as in Pd/MWCNT) is diffusion-controlled in the scan-rate range from 50 to 500 mV s^{-1}.[41,58]

Pd nanoparticles supported on benzenesulfonic-modified MWCNTs (S-MWCNTs) have been found to be more active for ethanol oxidation, less sensitive to CO poisoning, and more stable with time as compared to untreated Pd/MWCNT.[33] Likewise, excellent results for ethanol oxidation, especially in terms of catalyst stability, have been obtained by the treatment of MWCNTs with hydrofluoric acid.[37] A comparative CV study of Pd/MWCNT$_{HF}$ and Pd/MWCNT shows, in fact, that the enlarged micropores on the HF-treated nanotube walls can anchor the metal nanoparticles so effectively to overcome their agglomeration or unfastening from the support surface. Figure 13a reports the plots of the mass activity against the cycle numbers for the ethanol oxidation on Pd/MWCNT and Pd/MWCNT$_{HF}$, showing that the electrocatalytic activity of Pd/MWCNT$_{HF}$ is over two times higher than that of Pd/MWCNT at comparable Pd loading. Moreover, the Pd/MWCNT$_{HF}$ electrocatalyst is extremely stable with no significant degradation over 8000 cycles (Figure 13b), while the activity of Pd/MWCNT is reduced by 30% after 7000 cycles.

The CVs of ethanol oxidation on Pd/MWCNT and Pd/MWCN$_{THF}$ electrodes are shown in parts c and d, respectively, of Figure 13.

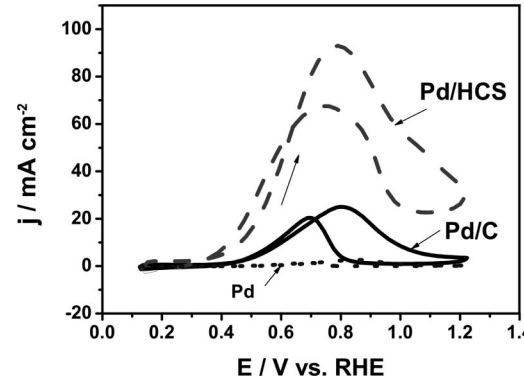

Figure 14. Cyclic voltammograms of ethanol oxidation on Pd/C and Pd/HCS in 1.0 mol dm^{-3} KOH/1.0 mol dm^{-3} ethanol solution at 303 K: scan rate, 50 mVs^{-1};. Pd loading, 300 μg cm^{-2}. Image is from ref 47.

The capacity of the support material to allow for a fast diffusion of the substrate has been invoked to explain the excellent behavior of a Pd/HCS electrode for the oxidation of ethanol (Figure 14).[47] Indeed, the HCS support exhibits a very high surface area (up to 1249 m^2 g^{-1} using the surfactant P123) as well as a much higher electrochemical active surface area (10.718 mC cm^{-2}) as compared to Pd/C or Pd metal (1.913 and 0.287 mC cm^{-2}, respectively).

3.1.2. Pd Electrocatalysts Mixed with Metal Oxides Supported on Carbon Blacks or Other Carbon Materials

Shen and Xu have been the first authors to demonstrate that the electroless reduction of $PdCl_2$ adsorbed onto oxide/C materials (oxide = CeO_2, Co_3O_4, Mn_3O_4, NiO) yields electrocatalysts for alcohol oxidation with much higher

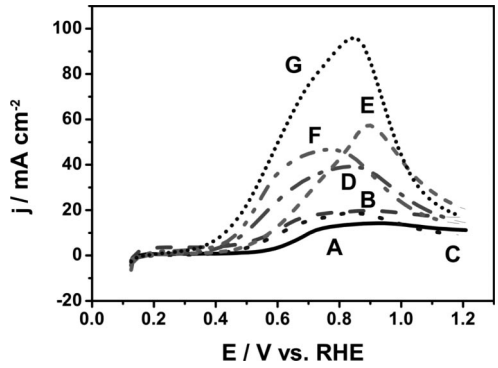

Figure 15. Anodic oxidation curves of ethanol on different Pd-oxide/C catalysts in 1.0 mol dm^{-3} ethanol/1.0 mol dm^{-3} KOH solution at 50 mV s^{-1}: (A) E-Tek Pt/C; (B) E-Tek PtRu/C; (C) Pd/C; (D) Pd-CeO_2/C; (E) Pd-Co_3O_4/C; (F) Pd-Mn_3O_4/C; (G) Pd-NiO/C. Pd loading: 300 μg cm^{-2}. Temperature: 303 K. Taken from ref 25.

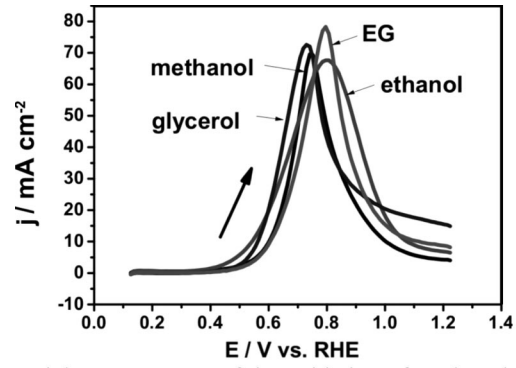

Figure 16. Linear potential sweep curves of the oxidation of methanol, ethanol, glycerol, and ethylene glycol on the as-prepared three-dimensional Pd/CPAA electrode in 1.0 mol dm^{-3} alcohol/1.0 mol dm^{-3} KOH solution at 25 °C: Pd loading, 300 μg cm^{-2}; scan rate, 50 mV s^{-1}. Image is from ref 73.

catalytic activity (onset oxidation potential and peak current density) (Figure 15) and electrochemical stability than any Pd/C or Pt/C catalyst under comparable experimental conditions.[25,52,53]

Various alcohols, including methanol, ethanol, glycerol, and ethylene glycol, are effectively oxidized on Pd-oxide/C electrodes. Out of all the electrocatalysts investigated, Pd-Co_3O_4 (2:1, w:w)/C shows the highest activity for the electrooxidation of methanol, ethylene glycol, and glycerol, while the most active catalyst for the ethanol electrooxidation is Pd-NiO (6:1, w:w)/C. On the other hand, Pd-Mn_3O_4/C shows significantly better performance stability than any other oxide-promoted Pd/C for the alcohol electrooxidation. It has been observed that the amount of metal oxide affects the catalytic activity as well as the electrode stability. In general, high contents of metal oxides reduce the electronic conductivity due to their semiconductor behavior, while, in some cases, the solubility of the metal oxides in alkaline solution can decrease the electrode stability, as is the case of the Pd-Co_3O_4/C electrocatalyst.[51]

Shen and co-workers have observed that the onset potential for ethanol oxidation on a Pd-NiO/C electrode is more negative and also provides a higher peak current density as compared to the case for a similar Pt-NiO/C electrode.[54] Also, it was found that the oxidation of CO on Pd-NiO/C exhibits a higher overpotential than that on Pt-NiO/C, whereas the peak area of CO oxidation on Pd-NiO/C is much smaller. Extensive potential oscillation occurs on Pt-NiO/C already at relatively low current densities and increases with the current density, which is a typical phenomenon of catalyst poisoning. Consistently, this electrode exhibits a much larger potential polarization as compared to the Pd-NiO/C electrode, which is stable even at relatively high current densities. Apparently, no strongly adsorbed species is formed on the Pd-NiO/C surface to block the active sites for ethanol oxidation. The drastic potential increase, up to the oxygen discharge, exhibited by the Pd-NiO/C electrode at 12 mA cm^{-2} has been attributed to a concentration polarization effect.[54]

An oxide of great influence on the electrochemical activity of Pd nanoparticles is In_2O_3, particularly in conjunction with MWCNTs as conductive support material.[72] In particular, it has been reported that a composite electrode with a mass ratio of Pd to In_2O_3 of 10:3 (Pd loading of 0.2 mg cm^{-2}) is twice as much more active than Pd/MWCNT.

A beneficial effect of the support material on the substrate diffusion has been observed for the oxidation of various alcohols (methanol, ethanol, ethylene glycol, and glycerol) on Pd electrocatalysts where a carbon black is replaced by either carbonized porous anodic alumina (CPAA)[73] or carbonized TiO_2 nanotubes (TiO_2C).[74] As shown in Figure 16, the Pd/CPAA electrode is quite active for the oxidation of all the alcohols investigated.

The better performance of the Pd/CPAA electrode as compared to the Pd/C electrode has been attributed to the improved mass transport of the alcohols across the micropores and mesopores bimodal structure of the material supporting the Pd catalyst on the former electrode.[73]

Quite similar results, in terms of both electrochemical activity and stability, have been reported for the ethanol oxidation on Pd/TiO_2C.[74] This electrocatalyst shows a higher surface area as well as higher electrochemical activity and stability as compared to Pd/C with the same metal loading. The best performance is provided by the Pd/TiO_2C catalyst with a Pd to TiO_2C ratio of 1:1. The onset potential of the ethanol oxidation on the Pd/TiO_2C electrocatalyst shows a negative shift of about 150 mV and a 3-fold peak current density as compared to Pd/C (Figure 17a).

The superior performance of Pd/TiO_2C has been attributed to the higher surface area originated by the porous structure of the TiO_2 nanotubes. Simple experiments such as plotting the scan rate against the ratio between the integrated charge of the anodic peak at different scan rates (Q_x) and the maximum charge at the scan rate of 5 mV s^{-1} (Q_{max}) (Figure 17b) or plotting the peak current density against the square root of the scan rate (inset of Figure 17b) showed that the mass transfer across the Pd/TiO_2C electrode is much faster than that across the Pd/C electrode so that the oxidation of ethanol at low scan rates on the former electrode is controlled by the activation polarization.

Hu and Shen have reported that Pd nanoparticles supported on hexagonal tungsten carbide single nanocrystals, successively mixed with Vulcan XC-72, are much more active than Pd/C for the oxidation of ethanol and have invoked a sort of synergistic effect to explain this phenomenon.[48] In Figure 18 are compared the CVs of Pd-WC/C and Pd/C for the ethanol oxidation in alkaline solution at room temperature. The Pd-WC/C electrocatalyst is significantly more active than Pd/C in terms of both negative onset potential and higher peak current density. Interestingly, the forward peak potential and the backward peak potential are very close to each other

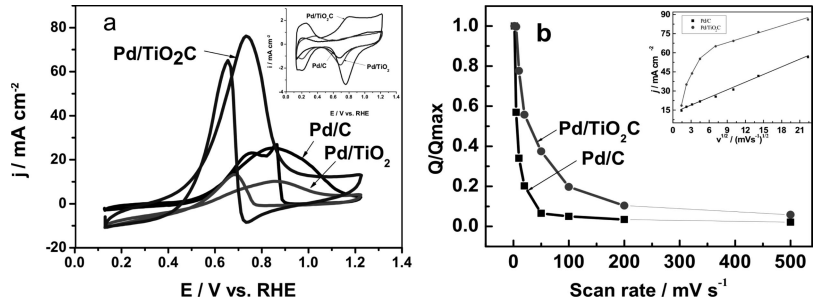

Figure 17. (a) Cyclic voltammograms of ethanol oxidation on Pd/C, Pd/TiO_2, and Pd/TiO_2C in 1.0 mol dm^{-3} KOH/1.0 M ethanol solution at 303 K: scan rate, 50 mVs^{-1}. Inset is the CVs in ethanol-free 1.0 mol dm^{-3} KOH solution to be used to compare the surface area. (b) Plot of normalized charge of anodic peak vs scan rate on Pd/C and Pd/TiO_2C electrodes. Inset is the plots of the peak current density against the square root of scan rate for both electrodes. Images are from ref 74.

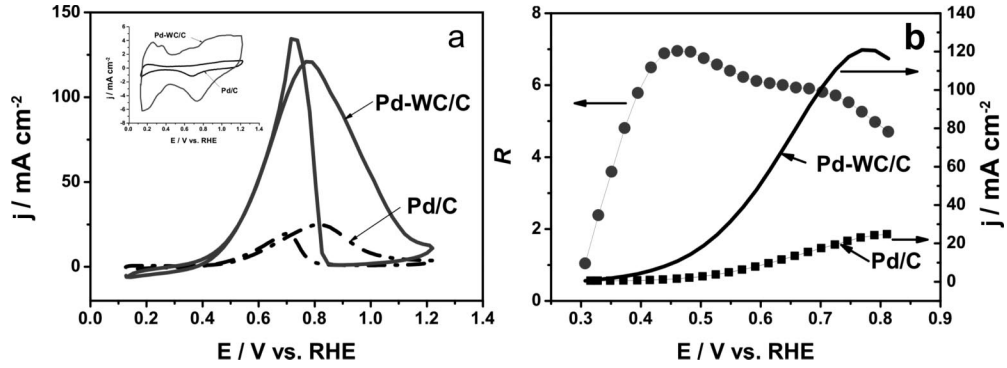

Figure 18. (a) Cyclic voltammograms of ethanol oxidation on Pd/C and 50 wt % Pd-WC/C in 1.0 mol dm^{-3} KOH/1.0 mol dm^{-3} M ethanol solution at 303 K: scan rate, 50 mV s^{-1} (inset is the cyclic voltammograms of Pd/C and 50 wt % Pd-WC/C in 1.0 mol dm^{-3} KOH). (b) Forward potential sweep curves of ethanol oxidation on Pd/C and 50 wt % Pd-WC/C (right) and the ratio *R* (left) between that of Pd-WC/C and Pd/C. Images are from ref 49.

on Pd-WC/C, which indicates a faster recovering of the electrode activity as compared to the Pd/C electrode, hence the ability of the Pd-WC/C electrode to sustain a higher potential polarization. Moreover, the inset of Figure 18a, illustrating the CVs of the two electrodes in 1.0 mol dm^{-3} KOH solution, proves that Pd-WC/C has a higher EASA than Pd. The *R* values reported in the ordinates of Figure 18b represent the ratio between the current densities on the Pd-WC/C and Pd/C electrodes at a certain potential. Notably, the *R* values are quite large, over 5, between +0.42 and +0.77 V vs RHE, which is a favorable characteristic for a fuel cell catalyst. Better results for ethanol oxidation have been obtained by the same authors with WC-modified Pd nanoparticles supported on MWCNTs (Pd-WC/MWCNT).[51] It has been suggested that the ethanol oxidation on Pd-WC/MWCNT is promoted both by the superior properties of the MWCNTs as compared to Vulcan XC-72 and by a synergistic effect between Pd and WC.[55] In this respect, it is worth mentioning that the combination of Pd nanoparticles with WC also improves the Pd resistance to CO poisoning.[48]

3.1.3. Pd Alloyed or Aggregated with Other Metals Supported on Carbon Blacks

The combination of Pd with other metals to give either alloys or aggregates has been intensively studied over the past few years with the aim of increasing the catalyst activity and stability as well as reducing the cost of the catalyst by diluting Pd with non-noble metals. Active Pd alloys for alcohol oxidation include PdPt,[27,62,68] PdAu,[31,48,64,75] and PdNi.[40,63]

Quite efficient PdPt/C electrocatalysts for the oxidation of ethylene glycol in alkaline solution have been prepared by Coutenceau et al.[26] These authors have also studied the effect of the Pd:Pt ratio and of the overall metal loading on the electrode, discovering that the highest activity is attained with a 20% metal loading and a 1:1 PdPt ratio. Besides being more active than commercial (E-TEK) bimetallic catalysts, the PdPt catalysts also exhibit a more negative potential shift. Likewise, In particular, the addition of Au to Pd/C significantly promotes the catalytic activity for the electrooxidation of 2-propanol and also increases its stability.[75]

The ethanol oxidation reaction on the catalysts Pd-(Ni-Zn)/C and Pd-(Ni-Zn-P)/C, obtained by the spontaneous deposition of Pd onto Vulcan XC-72-supported Ni-Zn or Ni-Zn-P alloys (*vide supra*), has been investigated by Bianchini and co-workers.[58] Figure 19 shows the CVs acquired at very low Pd loading (22 μg cm^{-2}) in 2.0 mol dm^{-3} KOH solution.

The Pd-(Ni-Zn-P)/C and Pd-(Ni-Zn)/C catalysts outperform any known anode electrocatalyst for the ethanol oxidation in half cells, especially in terms of specific current densities which are higher than 3600 Ag Pd^{-1}.[58] In addition, electrodes coated with Pd-(Ni-Zn)/C and Pd-(Ni-Zn-P)/C exhibit an excellent stability for the oxidation of ethanol, as shown by chronopotentiometry experiments. After some potential oscillation in the first 2−3 h of ethanol oxidation, the potential increases by only a few tens of millivolts after a further 5.5 h, which suggests the absence of effective catalyst deterioration, for example by the formation of strongly adsorbed species on the catalysts surface. CO poisoning has been ruled out as the factor responsible for the increase in the response potential exhibited by the Pd-(Ni-Zn)/C and Pd-(Ni-Zn-P)/C electrodes, as the corresponding catalysts are selective for the oxidation of ethanol

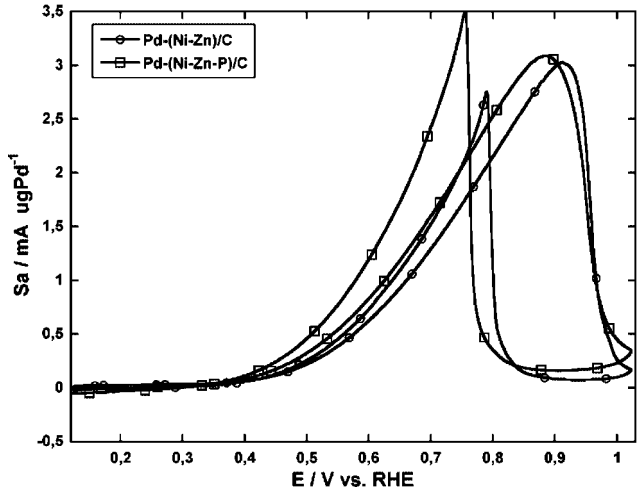

Figure 19. Cyclic voltammograms of ethanol oxidation on Pd-(Ni-Zn-P)/C and Pd-(Ni-Zn)/C electrodes in 2.0 mol dm^{-3} KOH and 10 wt % ethanol: Pd loading, 22 μg cm^{-2}; scan rate, 50 mV s^{-1}; room temperature. Image is from ref 58.

to acetate in strongly alkaline media (*vide infra*). The overpotentials have been attributed to other phenomena at the electrode interphase, including the increased viscosity of the solution, resulting in (i) a slower diffusion rate of ethanol, (ii) the decreased concentration of OH^- anions, and (iii) the competitive adsorption of the acetate ion on the active metal sites. Unlike ethanol oxidation, chronopotentiometric experiments of methanol and glycerol oxidation on Pd-(Ni-Zn)/C and Pd-(Ni-Zn-P)/C electrodes show a remarkable increase of the overpotential with time, with the oxygen discharge potential being attained after 2.5 and 1.5 h with methanol and glycerol, respectively.[76] In addition to decreasing the electrochemical stability of the electrodes, the oxidation of methanol and glycerol on Pd-(Ni-Zn)/C and Pd-(Ni-Zn-P)/C is also much slower than that of ethanol under comparable experimental conditions, as shown by the corresponding CVs illustrated in Figure 20.

The high dispersion of the Pd clusters and the presence of single Pd sites on the surface of Pd-(Ni-Zn)/C and Pd-(Ni-Zn-P)/C have been suggested to be important factors in boosting the electrocatalytic performance of these materials.[58] On the other hand, although independent CV experiments in KOH solution with Ni-Zn/C and Ni-Zn-P/C electrodes, prior to and after alcohol addition, have excluded any direct role of the Ni support, the existence of a cocatalytic effect of Ni on the Pd-catalyzed oxidation reaction of alcohols has not been disregarded. Indeed, the copresence of nickel or nickel oxide may have a beneficial effect on the electro-oxidation of alcohols on transition metals in either acidic or alkaline media (*vide infra*).[25,53,77,80]

3.1.4. Pd-Based Electrocatalysts Unsupported or Supported on Noncarbonaceous Materials

Unsupported Pd electrodes are mostly used for fundamental research. Wang et al. have studied the electrocatalytic activity of Pd nanowire arrays, finding that the Pd NWA electrode is much more active for the electrooxidation reaction of ethanol than either a Pd film or a PtRu/C catalyst (Figure 21).[66,67] In particular, the onset oxidation potential on the Pd NWA electrode (+0.35 V) is 170 mV more negative than that on the Pd film electrode (+0.52 V) and 40 mV more negative than that on a E-TEK PtRu/C electrocatalyst (+0.39 V). Notably, the anodic peak current on the Pd NWA electrode (74 mA cm^{-2} with a Pd loading of 1.1 mg cm^{-2}) is seven times larger than that provided by the Pd film electrode and almost double that provided by the PtRu/C electrode.

Tong and co-workers have investigated the oxidation of methanol, 1-propanol, and 2-propanol on electrodes constituted by Pt and Pd disks, discovering that, in alkaline media, Pd is a much better catalyst for the oxidation of 2-propanol and 1-propanol as compared to Pt.[81]

Palladium electrocatalysts supported on other materials than carbon blacks constitute a small but rather interesting family with great potential also in water electrolysis. Of particular interest are the materials described by Li et al. where Pd nanoparticles are supported on either β-MnO_2 nanotubes (Pd/β-MnO_2)[44] or VO_x nanotubes (Pd/VO_x).[43] A study of methanol oxidation in NaOH solution showed that both Pd/β-MnO_2 and Pd/VO_x are better catalysts than traditional Pd/C catalysts at comparable metal loading.[43,44]

Zheng et al. have reported the preparation of PdPt electrocatalysts by the partial spontaneous replacement of Pt on Pd film and have shown that PdPt on indium−tin oxide (ITO) is much more active for ethanol oxidation than Pd/ITO.[62] Likewise, a PdRu/Ni electrocatalyst has been reported to have a more negative onset oxidation potential for ethanol oxidation and a higher tolerance to adsorbates as compared to a PtRu/Ni electrocatalyst.[82]

3.2. Direct Alcohol Fuel Cell Performance

Essential components of any MEA for a DAFC are the anode and cathode electrodes and the solid electrolyte, generally constituted by an ion-exchange membrane, that,

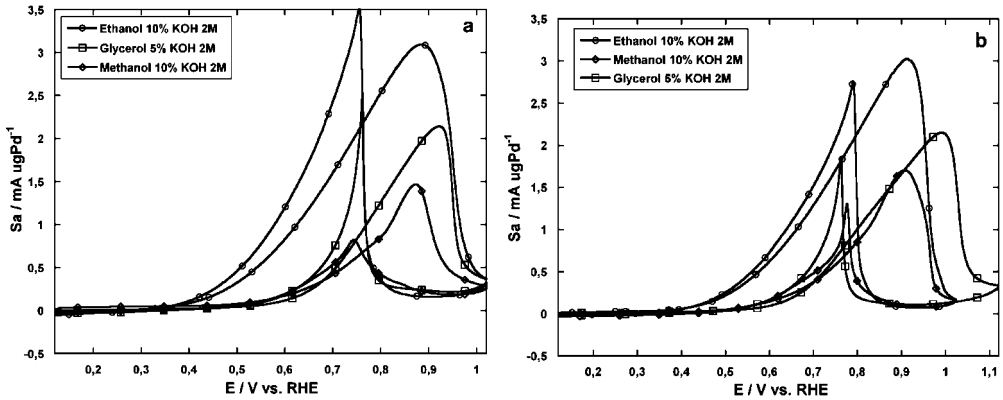

Figure 20. Cyclic voltammograms of methanol, ethanol, and glycerol oxidation on Pd-(Ni-Zn)/C (a) and Pd-(Ni-Zn-P)/C (b) electrodes in 2.0 mol dm^{-3} KOH: Pd loading, 22 μg cm^{-2}; scan rate, 50 mV s^{-1}; room temperature. Images are from refs 58 and 76.

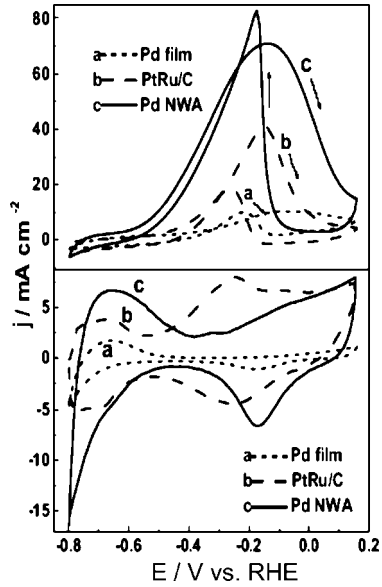

Figure 21. Cyclic voltammograms measured on a Pd film electrode (curve a; Pd loading, 1.1 mg cm^{-2}), an E-TEK PtRu (2:1 by weight)/C electrode (curve b; Pt loading, 0.24 mg cm^{-2}), and a Pd NWA electrode (curve c; Pd loading, 0.24 mg cm^{-2}) in 1.0 mol dm^{-3} KOH + 1.0 mol dm^{-3} mL C_2H_5OH (upper panel) and 1.0 mol dm^{-3} KOH (lower panel) solution at a scan rate of 50 mV s^{-1}. Image is from ref 66.

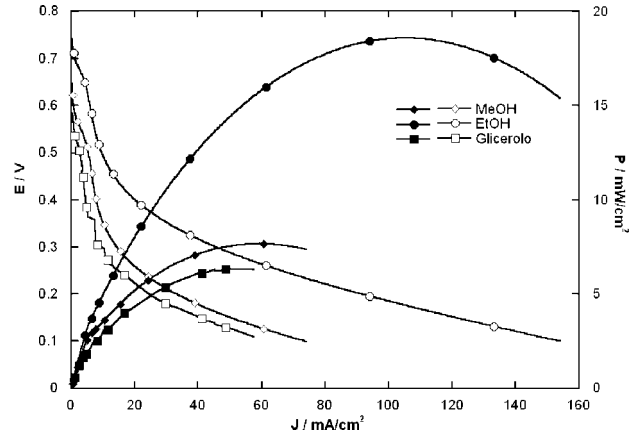

Figure 22. Polarization and power density curves provided by a oxygen-breathing DAFC fueled with 2 mol cm^{-3} KOH solutions of methanol (10 wt %), ethanol (10 wt %), or glycerol (5 wt %) at 20−22 °C containing a MEA with a Pd/MWCNT anode, a Hypermec K-14 Fe-Co cathode, and a Tokuyama A006 membrane. Pd loading on the anode: 1 mg cm^{-2}. Image is from ref .

besides allowing for the passage of ions from one compartment to the other, serves to insulate the electrodes so as to avoid short circuits. The MEAs are used to fabricate the monoplanar cells which exist as passive or active systems. In the passive systems, the cathode is exposed either to air or to a static oxygen atmosphere (air- or oxygen-breathing cathode) at room temperature, while in the active systems air or, more often, oxygen is provided at a certain pressure and dynamic flow (mL min^{-1}) and the temperature is controlled instrumentally. Likewise, the anodes of the passive systems are directly exposed to an alkaline aqueous solution of the desired alcohol, while, in the active DAFCs, the fuel is supplied at controlled flow and temperature.

All the anodes of the DAFCs described below contain a Pd-based catalyst among those described in previous pages, while the cathodes are generally manufactured with commercial catalysts. In between anode and cathode there is an anion-exchange membrane (AEM) and the fuel solution is generally made strongly alkaline by the addition of a base such as KOH or NaOH. The rationale of the application of AEMs as electrolytes in the DAFCs with Pd-catalyzed anodes has been illustrated in previous sections of this article. It is worth stressing here that most of the AEMs employed in the DAFCs reviewed below are commercial products from Tokuyama Co. or Solvay. To the best of our knowledge, no homemade membrane, of which there are many interesting examples,[10−21] has ever been used in a DAFC where the anode catalyst is based on Pd.

3.2.1. Passive DAFCs

Very few examples of passive DAFCs have been reported so far in the open literature. Most researchers are apparently inclined to work with active systems for their better control of the experimental parameters. On the other hand, passive cells are much easier to fabricate and handle and can provide fast and reliable information, especially as regards the nature and concentration of the alcohol oxidation products as well as the extent of the alcohol crossover. In fact, the anode compartment can be sealed under an inert atmosphere so as to allow for a reliable quantitative analysis of the fuel retained and of the cell products using various techniques (ion chromatography, HPLC, NMR spectroscopy, GC-MS).

Passive DAFCs equipped with an anion-exchange membrane and a Pd-based anode electrocatalyst have been recently described.[26,27,41,58,76] A detailed description of the cell hardware used has also been reported.[41] The MEAs comprise Fe-Co Hypermec K-14 cathodes by ACTA SpA,[80] a Tokuyama A-006 membrane, and Ni foam anodes coated with Pd/MWCNT, Pd-(Ni-Zn)/C, or Pd-(Ni-Zn-P)/C (*vide supra*).[41,58]

The polarization and power density curves obtained on DAFCs containing Pd/MWCNT anodes and fueled with methanol, ethanol, and glycerol in 2 mol cm^{-3} KOH solutions at room temperature are reported in Figure 22. Prior to recording these curves, the cells were conditioned at the OCV for 1 h. Under these conditions, ethanol shows the highest open circuit voltage (OCV, 0.74 V) as well as the highest peak power density (18.4 mW cm^{-2} at 0.2 V).[41] This performance trend is different from that observed in the half cell, where glycerol gives the highest peak current density (Figure 12), but it is fully consistent with the chronopotentiometric experiments. This confirms that the oxidation of MeOH and glycerol on Pd/MWCNT leads to intermediate products, CO and hydroxyacids, respectively, whose further oxidation or desorption is difficult to achieve.

The power density provided by the DMFC (8 mW cm^{-2}) at room temperature matches well the value reported by Coutanceau et al. for a cell fueled with a 1 mol cm^{-3} MeOH/1 mol cm^{-3} NaOH solution, containing an ADP-type membrane from Solvay and an anode coated with 2 mg cm^{-2} of PtPd/C.[26]

To the best of our knowledge, no example of a passive *direct glycerol fuel cell* (DGFC) with a Pd anode electrocatalyst has been reported so far in the literature. The power density of the Pd/MWCNT cell described by Bianchini, however, is comparable to that of the *direct ethylene glycol fuel cell* (DEGFC) realized by Coutanceau et al. (2 mol cm^{-3} ethylene glycol in a 4 mol cm^{-3} NaOH solution) containing a $Pt_{0.45}Pd_{0.45}Bi_{0.5}$/C anode catalyst (overall metal loading 2

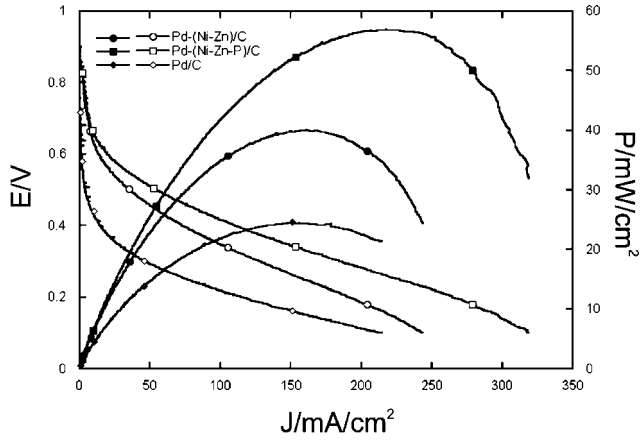

Figure 23. Polarization and power density curves provided by oxygen-breathing DEFCs fueled with 2 mol cm^{-3} KOH solutions of ethanol (10 wt %) at 20−22 °C containing MEAs with Hypermec Fe-Co cathodes, a Tokuyama A006 membrane, and Pd-(Ni-Zn)/C, Pd-(Ni-Zn-P)/C, or Pd/C anodes: Pd loading, 1 mg cm^{-2}.[76b]

mg cm^{-2}).[27] Coutanceau has also observed that palladium exhibits lower activity for ethylene glycol (EG) oxidation than platinum, especially in terms of onset oxidation potential, while the addition of Pd to a PtBi catalyst increases the current density without changing the onset potential. The beneficial effect of Pd has been attributed to the ability of this metal to disfavor C−C bond breaking reactions (increased production of oxalate), thus reducing electrode poisoning by CO_{ads}.[27]

Much better performances, especially in terms of peak power densities, have been recently obtained with DEFCs containing Ni foam anodes coated with the Pd-(Ni-Zn)/C and Pd-(Ni-Zn-P)/C electrocatalysts.[58,76b] As shown in Figure 23, these catalysts are extremely active also at room temperature and at low Pd loading (1 mg cm^{-2}), providing up to 60 mW cm^{-2} at 0.3 V, which is the highest value ever reported for a DEFC at room temperature. Indeed, a peak power density of 27 mW cm^{-2} at 25 °C has been obtained with an AFC containing a 3 mol cm^{-3} KOH solution as electrolyte and an anode coated with 1 mg cm^{-2} of Pt-black.[83] Figure 23 reports also the polarization and power density curves exhibited by a DEFC containing a Pd/C anode catalyst obtained by reduction with EG of Vulcan XC-72-adsorbed $PdCl_2$.[58,76b] The Pd/C electrocatalyst is apparently much less efficient, especially in terms of potential output and electrochemical stability, than the Pd-(Ni-Zn)/C and Pd-(Ni-Zn-P)/C electrocatalysts.

Galvanostatic experiments have been carried out at room temperature on the DEFCs containing Pd/MWCNT, Pd-(Ni-Zn)/C, Pd-(Ni-Zn-P)/C, or Pd/C anodes as well as on DMFCs and DGFCs containing a Pd/MWCNT anode. These experiments have provided valuable information on the level of alcohol oxidation, the alcohol crossover, and the total cell efficiency.

As a standard procedure, the anode compartments were filled with 28.3 mmol of EtOH, 40.7 mmol of MeOH, or 6.8 mmol of glycerol. $^{13}C\{^1H\}$ NMR spectroscopy and ionic chromatography, using reference materials and calibration curves, was used to analyze the contents of the anode compartments after each galvanostatic experiment.

Irrespective of the Pd catalyst, the analyses of the DEFC exhausts were unequivocally consistent with the selective

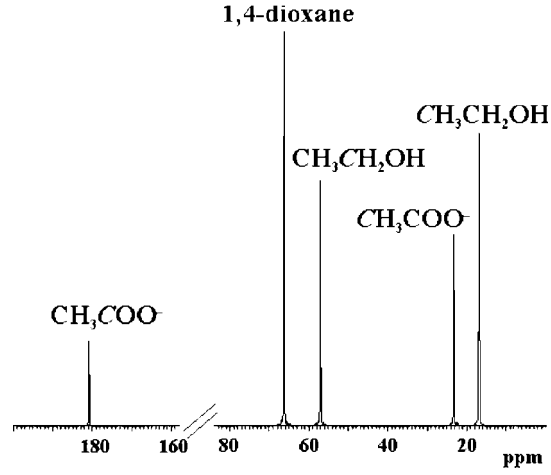

Figure 24. $^{13}C\{^1H\}$ NMR spectrum at room temperature of the anode solution of DEFC with a Pd/MWCNT anode after supplying 102 mA for 12.5 h. Image is from ref .

oxidation of ethanol to acetate at the anode so that the anode reaction can be described by eq 1.

$$C_2H_5OH + 5OH^- \rightarrow CH_3COO^- + 4H_2O + 4e^- \quad (1)$$

After a conditioning time of 1 h at the OCV, the DEFC with the Pd/MWCNT anode was subjected to a constant current of 102 mA until zero voltage. Under these conditions, the DEFC gave 102 mA for 12.5 h to form 12 mmol of acetate (isolable as potassium acetate), leaving 12 mmol of unreacted ethanol.[41] The $^{13}C\{^1H\}$ NMR spectrum of the corresponding cell exhausts is shown in Figure 24. Under comparable experimental conditions, the DEFCs with the Pd-(Ni-Zn)/C and Pd-(Ni-Zn-P)/C anodes supplied 102 mA for 10.9 and 10.4 h, producing 10 and 9.6 mmol of acetate, respectively, at remarkably higher potentials than those provided by the Pd/MWCNT anode.[71,76a] Approximately 4 mmol of EtOH were lost by evaporation irrespective of the anode catalyst. Since the anode compartments were accurately sealed during the experiments, the fuel losses have been attributed mostly to the evaporation of the crossover ethanol from the cathode side.

It is worth stressing that the DEFCs with the Pd-(Ni-Zn)/C and Pd-(Ni-Zn-P)/C anodes can be fully regenerated (same OCV and galvanostatic performance) upon replacement of the cell exhausts with fresh 2 mol cm^{-3} KOH solutions of ethanol. This procedure was repeated several times with no apparent performance decay. In view of these results, the observed polarizations have been ascribed to other factors than catalyst or electrode poisoning, i.e. the increasing viscosity of the solutions, the decreased OH^- concentration, and the competitive adsorption of substrate/partial oxidation product on the catalyst surface.

Notably, a power density of 1.1 mW cm^{-2} at 1.4 V is supplied by a passive four-cell stack with 5 cm^2 MEAs constituted by a Pd-(Ni-Zn)/C anode, a Fe-Co Hypermec K-14 cathode, and a Tokuyama A-006 membrane at 25−30 °C.[76b] This stack, equipped with a step-up converter, suffices to charge the battery of any portable phone and is comparable in performance to a two-cell PEMFC device with the hydrogen supplied by a water-aluminum microgenerator.[84]

Under comparable conditions to those of the DEFCs described above, the DMFC with the Pd/MWCNT anode

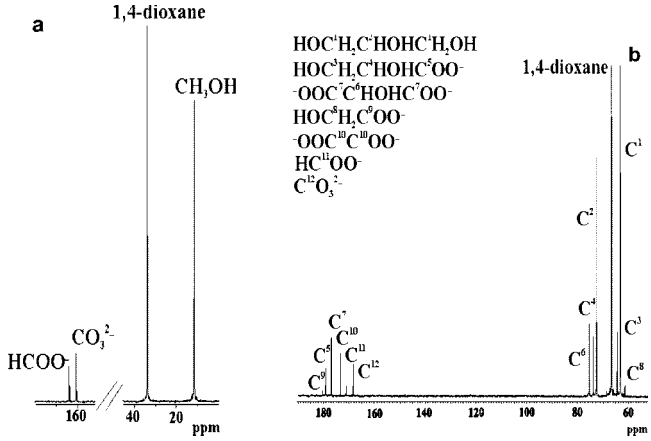

Figure 25. $^{13}C\{^1H\}$ NMR spectrum at room temperature of the anode solution of (a) a DMFC with a Pd/MWCNT anode supplying 102 mA for 10.3 h and (b) a DGFC with a Pd/MWCNT anode supplying 102 mA for 8.4 h. Images are from ref 41.

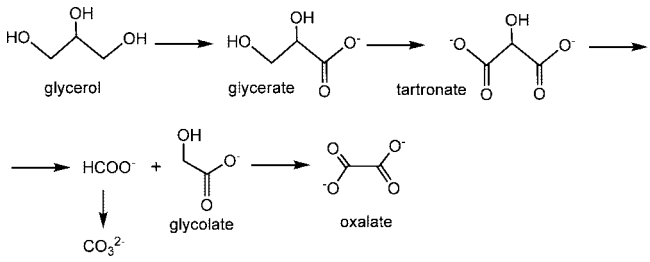

Figure 26. Products obtained by the partial oxidation of glycerol on Pd/MWCNT anodes in a passive DGFC.[41]

kept on working for 10.3 h, yielding 3 mmol of formate and 7 mmol of carbonate with 22 mmol of unreacted MeOH (Figure 25a).[41] The anode oxidation reactions occurring in the DMFCs are reported in eqs 2−4. The loss of substrate was therefore ca. 8 mmol, in line with the lower boiling point of methanol and its easier permeation through the membrane as compared to ethanol.

$$CH_3OH + 8OH^- \rightarrow CO_3^{2-} + 6H_2O + 6e^- \quad (2)$$

$$CH_3OH + 5OH^- \rightarrow HCOO^- + 4H_2O + 4e^- \quad (3)$$

$$HCOO^- + 3OH^- \rightarrow CO_3^{2-} + 2H_2O + 2e^- \quad (4)$$

The analysis of the DGFC exhausts of a passive cell equipped with a Pd/MWCNT anode showed the conversion of glycerol into various products which are illustrated in Figure 26.[41] The corresponding $^{13}C\{^1H\}$ NMR spectrum is shown in Figure 25b.

Overall, the DGFC provided current for 8.4 h, producing 3070 C and leaving 10 mmol of unreacted glycerol. About 4 mmol of glycerol was consumed to give glycolate (4%), glycerate (27%), tartronate (23%), oxalate (15%), formate (9%), and carbonate (22%). Consistent with the high boiling point and lower membrane permeability of glycerol, no appreciable loss of fuel was observed.

On replacement of the cell exhausts with fresh 2 mol cm^{-3} KOH solutions of methanol or glycerol, both the DMFC and the DGFC started working with only minor decay in the OCV and galvanostatic performance.

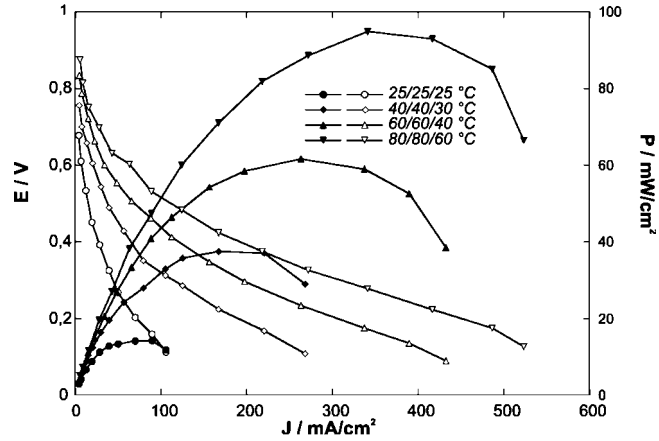

Figure 27. Polarization and power density curves at different temperatures of an active DMFC with a Pd/MWCNT anode (Pd loading, 1 mg cm^{-2}), fueled with an aqueous 2 mol cm^{-3} KOH solution of methanol (10 wt %). The inset reports the temperatures of fuel (left), cell (central), and oxygen gas (right). Image is taken from ref .

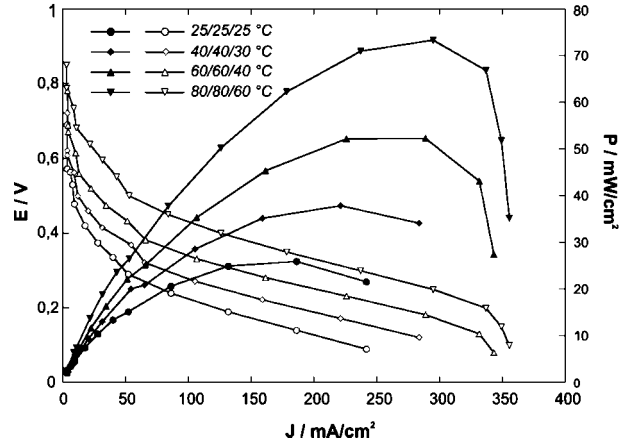

Figure 28. Polarization and power density curves at different temperatures of an active DEFC with a Pd/MWCNT anode (Pd loading, 1 mg cm^{-2}), fueled with an aqueous 2 mol cm^{-3} KOH solution of ethanol (10 wt %). The inset reports the temperatures of fuel (left), cell (central), and oxygen gas (right). Image is taken from ref .

3.2.2. Active DAFCs

Reports in the open literature on active DAFCs with Pd-based anode electrocatalysts are more rare than those on passive systems. However, as will be shown in forthcoming pages, their electrochemical performance may be so good that a near industrial application as power generators for portable electronics cannot be excluded.

Figures 27−30 show the polarization and power density curves of DAFCs with a MEA constituted by a Pd/MWCNT anode (1 mg cm^{-2} Pd on Ni foam), a Fe-Co Hypermec K-14 cathode, and a Tokuyama A-006 membrane.[41] These cells have been fed with 2 mol cm^{-3} KOH solutions containing 10 wt % methanol, 10 wt % ethanol, or 5 wt % glycerol at 4 mL min^{-1} with an oxygen flow at the cathode of 200 mL min^{-1}. The cell temperature was regulated at 25, 40, 60, or 80 °C.

In the temperature interval from 25 to 40 °C, the performance trend exhibited by the three DAFCs is analogous to that found for the passive cells, with the DEFC (Figure 27) being superior to both the DMFC (Figure 28) and the DGFC (Figure 29). On the other hand, increasing the cell

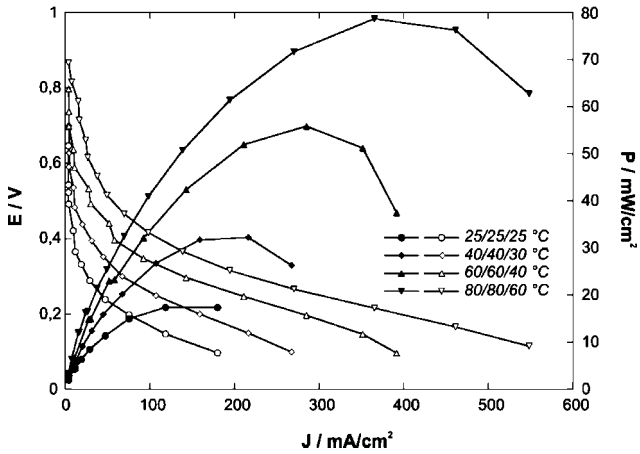

Figure 29. Polarization and power density curves at different temperatures of an active DGFC with a Pd/MWCNT anode (Pd loading, 1 mg cm^{-2}), fueled with an aqueous 2 mol cm^{-3} KOH solution of glycerol (5 wt %). The inset reports the temperatures of fuel (left), cell (central), and oxygen gas (right). Image is taken from ref .

temperature to 60 °C leads to a reverse order of activity, with the highest power density supplied by the DMFC (peak power density of 95 mW cm^{-2} at 80 °C) and the lowest peak power density supplied by the DEFC (73 mW cm^{-2} at 80 °C). The latter cell shows a sudden drop of voltage after 300 mA cm^{-2}, which has been attributed to a strong contribution of the concentration polarization. Below 300 mA cm^{-2} at 80 °C, the DEFC was competitive with the other cells. It has been suggested that the MWCNT support, rich in surface carboxylic acid groups,[69] may be responsible for the observed activity trend through a specific control of the substrate diffusion/product desorption. Indeed, among the partial oxidation products of glycerol (Figure 26), there are hydroxy acids and biacids that can interact with the surface carboxylic acid groups present on the MWCNT surface.

Indirect support for the role of the carbon support on the DAFC performance has been provided by further studies in the same laboratory showing that ethanol is a better fuel than methanol or glycerol at any temperature from 20 to 80 °C in identical cells except for those containing Pd-(Ni-Zn)/C or Pd-(Ni-Zn-P)/C anodes.[58,76] The polarization and power density curves of these DAFCs are shown in Figure 30. Quite comparable results have been obtained for DAFCs containing Pd-(Ni-Zn-P)/C anodes.[76]

All the peak power densities provided by these DAFCs, but especially those fed with ethanol, are extraordinarily high, up to 170 mW cm^{-2} at 80 °C and 125 mW cm^{-2} at 60 °C at 0.3 V (Figure 30a).

The selective conversion of ethanol to acetate occurred also in the active DEFCs with the Pd-(Ni-Zn)/C and Pd-(Ni-Zn-P)/C anodes as shown by the analysis of the anode exhausts after galvanostatic experiments at 60 °C. Figure 31 shows the galvanostatic trace of the DEFC with a Pd-(Ni-Zn)/C anode at a constant current of 100 mA. After a conditioning time of 1 h at the OCV of 0.75 V, the cell was monitored for more than 220 h, showing a modest 15% decay of the cell voltage. The overall conversion of ethanol to potassium acetate was 0.2 mol and was accompanied by the production of ca. 78160 C.

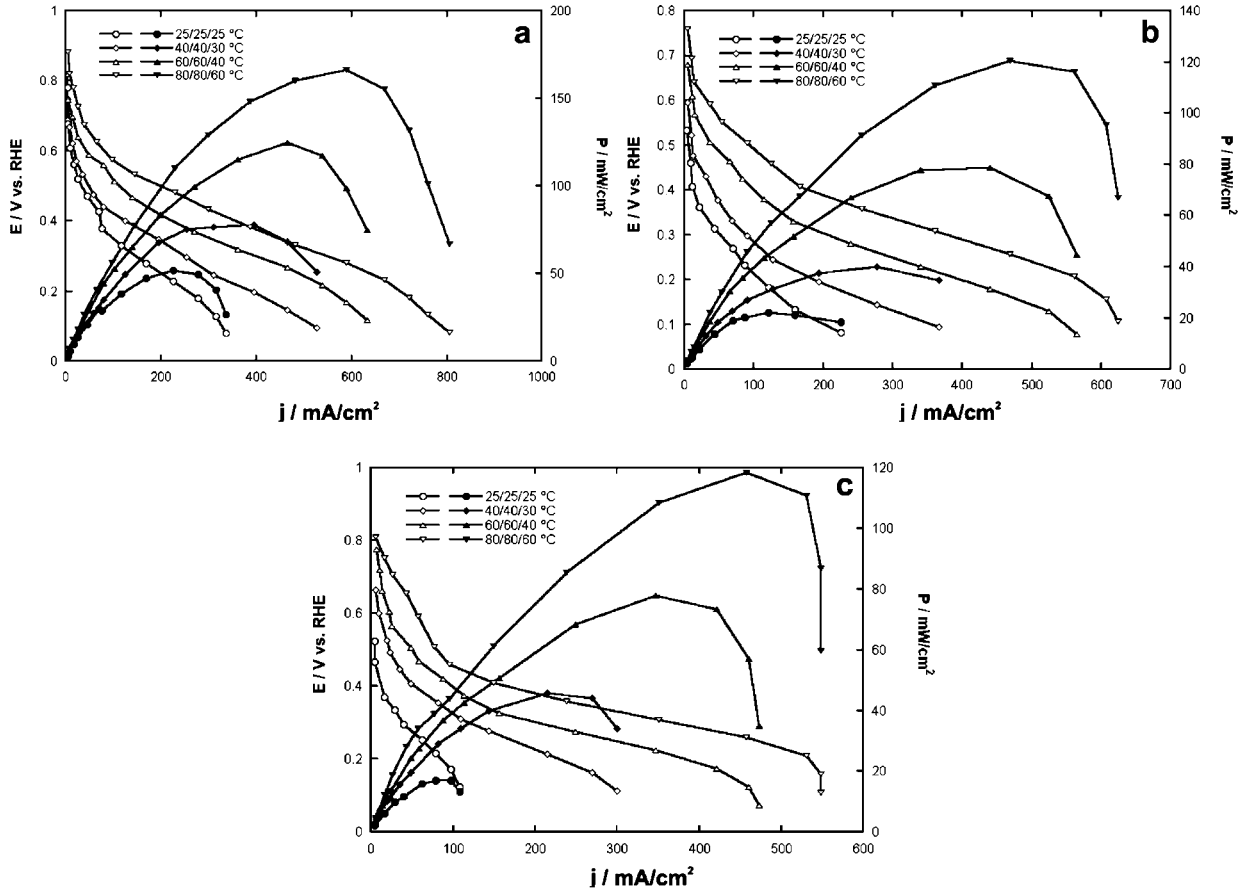

Figure 30. Polarization and power density curves at different temperatures of active DAFCs with Pd-(Ni-Zn)/C anodes fueled with aqueous 2 mol cm^{-3} KOH solutions of (a) ethanol (10 wt %), (b) methanol (10 wt %), and (c) glycerol (5 wt %): Pd loading, 1 mg cm^{-2}. The inset reports the temperatures of fuel (left), cell (central), and oxygen gas (right).[76]

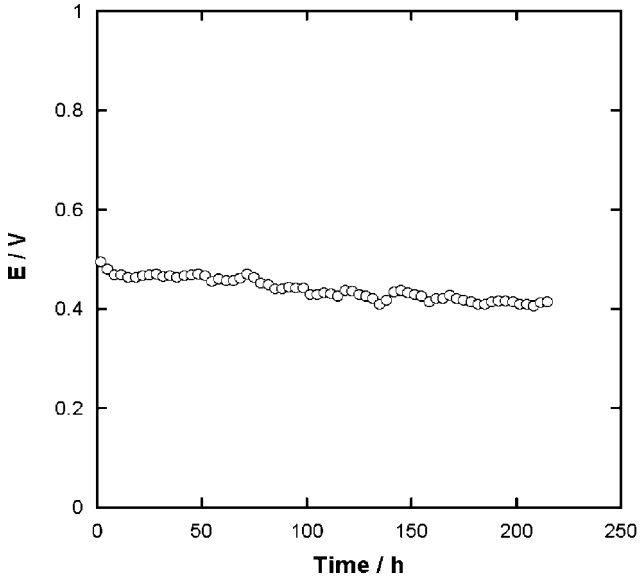

Figure 31. Galvanostatic trace at 60 °C and 100 mA of an active DEFC with a MEA constituted by a Pd-(Ni-Zn)/C anode (1 mg cm^{-2} Pd), a Fe-Co Hypermec K-14 cathode, and a Tokuyama A-006 membrane.[76]

Recent studies in our laboratories show that the Pd-(Ni-Zn)/C or Pd-(Ni-Zn)/C catalysts are much more selective than Pd/MWCNT for the oxidation of ethylene glycol and glycerol in active DAFCs at 60 °C.[76a] The former fuel is mostly converted to glycolate (>90%), and the latter to tartronate (>70%).

Some examples of active DAFCs with anion-exchange membranes have been described in the literature, but all of them contain Pt-based anode electrocatalysts and their performance is far lower than that of the DAFCs with Pd-based anode catalyst. Nevertheless, a survey of the most efficient active DAFCs of this type is given below for comparative purposes.

A Tokuyama A-006 membrane has been used by Bunawaza and Yamazaki in a DMFC with a PtRu/C anode and either Pt/C or Ag/C cathodes.[20] Even by using an anion ionomer and feeding the anode with a 1 mol cm^{-3} MeOH/0.5 mol cm^{-3} NaOH solution, the highest power density at 80 °C was <60 mW cm^{-2}, far away from the value of 120 mW cm^{-2} obtainable with the MEA constituted by the Pd-(Ni-Zn)/C anode, the Fe-Co Hypermec K-14 cathode, and the Tokuyama A-006 membrane (Figure 30a).

Ogumi et al. have reported on active DAFCs fed with 1 mol cm^{-3} KOH solutions of various alcohols and polyalcohols, including methanol and glycerol, but not ethanol.[85] The anode and cathode catalysts were PtRu/C (4 mg cm^{-2}) and Pt/C (1 mg cm^{-2}) from E-TEK (USA), respectively, and the solid electrolyte was a Tokuyama AHA membrane. The peak power densities at 45 °C with methanol and glycerol were 8 mW cm^{-2} at 28 mA cm^{-2} and 6 mW cm^{-2} at 27 mA cm^{-2}, respectively.

Scott et al. have investigated the performance of an active DMFC using a Morgane-ADP membrane from Solvay using PtRu/C (1 mg cm^{-2}) as anode catalyst and Pt/C as cathode catalyst (both from E-TEK).[16] At 60 °C using an oxygen flow, the highest power density was ca. 11 mW cm^{-2} at ca. 40 mA cm^{-2}.

An active alkaline DEFC has been described by Hou et al., where the anode and cathode were catalyzed by commercial (Johnson-Matthey) Pt-Ru/C (2 mg cm^{-2}) and Pt/C (1 mg cm^{-2}) catalysts, respectively, and the solid electrolyte was a polybenzylimidazole membrane doped with KOH, which is not a real anion-exchange membrane, however.[15] At 75 °C, a peak power density of 49 mW cm^{-2} was obtained that increased to 61 mW cm^{-2} by increasing the cell temperature to 90 °C.

Varcoe et al. have studied the performance of various proprietary anion-exchange membranes in DAFCs fueled with MeOH, EtOH, or EG with PtRu/C anodes.[12] The highest power density was obtained with MeOH (30.6 mW cm^{-2}), while the power densities provided by EtOH and EG were lower than 10 mW cm^{-2}.

In conclusion, the power density values, combined with the good electrochemical stability of the MEAs, give a mark of excellence to the active DEFCs with the Pd-(Ni-Zn)/C and Pd-(Ni-Zn-P)/C anodes, although one cannot disregard the contribution provided by the high quality of the cathode catalyst and of the anion-exchange membrane. In particular, Pd-(Ni-Zn)/C has been found to be more active than Pd-(Ni-Zn-P)/C, Pd/C, or Pd/MWCNT and, as such, exhibits unrivaled activity as anode electrocatalyst for alcohol oxidation in alkaline media. On the other hand, a great margin of improvement may be envisaged through the optimization of the electrode architecture as well as the use of an anion ionomer to reduce the ohmic and diffusion polarizations. The projected power density (on a stack basis with four 10 cm^2 cells) for these DEFCs operating at 80 °C is close to 6 W at 1.6 V, which is suitable to power a great variety of portable electronics, provided the use of a step-up converter.

Finally, it is also worth stressing that no known anode catalyst based on platinum, even at high metal loading, has demonstrated the capacity to produce acceptable power densities in active DAFCs equipped with a polymeric proton-exchange membrane. Apart from methanol, for which there exist platinum-based catalysts capable of producing current densities of several tens of mW cm^{-2},[4] the higher alcohols such as ethanol and polyalcohols such as glycerol are difficult to oxidize on platinum or platinum alloyed with either noble or non-noble metals, unless the temperature is increased to 130−150 °C, in which case, however, hybrid inorganic−organic proton-exchange membranes are used.[1,7] The best DEFC performances so far reported have been obtained at temperatures above 90 °C with binary PtSn and PtRu anode catalysts in conjunction with platinum-based cathodes and Nafion membranes.[1,86] However, the power densities never exceed 60−70 mW cm^{-2}, and the overall efficiency suffers the consequences of the partial oxidation of ethanol to mixtures of acetaldehyde, acetic acid, and CO_2, while severe overpotentials are generally originated by catalyst poisoning by CO.

4. Mechanistic Studies of Alcohol Oxidation on Pd-Based Electrocatalysts

Unlike the case for Pt-based electrocatalysts,[17,27,86−102] very few mechanistic studies on the oxidation of alcohols on Pd-based electrocatalysts have been reported and most of them are *ex-situ* analysis of cell exhausts.[26,41,54,58] The scarcity of reliable and cost competitive AEMs has certainly contributed to moderate the interest of many researchers in Pd-based electrocatalysts. With the advent of efficient and commercially available AEMs, together with the progress achieved in the development of new catalytic architectures, the situation has changed and the research on Pd-based anodes for DAFCs is now blossoming. Understanding the

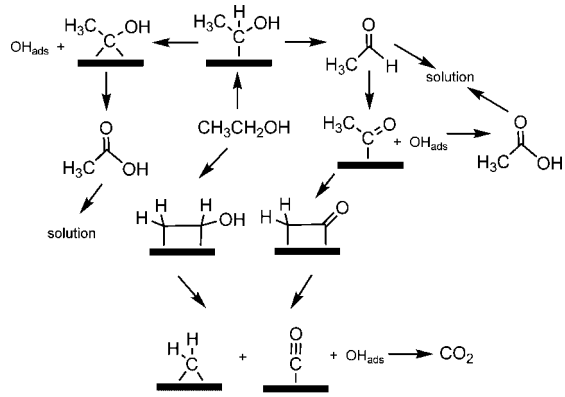

Figure 32. Proposed scheme for ethanol oxidation on Pt-based electrocatalysts in acidic media.

mechanism of alcohol oxidation in alkaline media is therefore a priority for the design and development of efficient MEAs for DAFCs.

It is generally agreed that all alcohols are oxidized following two distinct reaction paths: a path involving CO_{ads} intermediate and a path where C−C bond breaking does not occur. Even for methanol with a single carbon atom, these two paths are possible.[88,89] For the sake of clarity, however, the following survey of mechanistic studies will consider separately EtOH, MeOH, and poly-alcohols. Reference to mechanisms proved or hypotheses for Pt-based catalysts is given at the beginning of each section to provide the reader with "the state of the art" in a much more developed field.

4.1. Ethanol Oxidation on Pd-Based Electrocatalysts

A generally accepted reaction scheme for ethanol oxidation on Pt-based catalysts is shown in Figure 32.[17,94] The reaction mechanism is actually split into three paths leading to either acetaldehyde or acetic acid formation and a path leading to CO_2 formation. For each path, however, the low-potential activation of water by the electrocatalyst (eqs 5 and 6) is mandatory to accomplish both the oxidation of CO_{ads} to CO_2 and the C−O coupling that transforms $acyl_{ads}$ into acetic acid (Figure 32).

$$(OH_2)_{ads} \rightarrow (OH)_{ads} + H^+ + e^- \quad (5)$$

$$(OH)_{ads} \rightarrow (O)_{ads} + H^+ + e^- \quad (6)$$

$$(CO)_{ads} + (O)_{ads} \rightarrow CO_2 \quad (7)$$

Increasing the pH from acidic to alkaline does not seem to affect the outcome of methanol,[81,85] ethanol,[87] and ethylene glycol oxidation[27] on Pt-based electrocatalysts, at least as far as the product selectivity is concerned. In contrast, Pd-based electrocatalysts are active only in alkaline media, where they are also much more selective, due to their low propensity to cleave C−C bonds.

As shown in previous sections of this review, ethanol is selectively converted to acetate on Pd-based electrocatalysts on the condition that they do not contain Pt and the anode solution is strongly alkaline. In no case has acetaldehyde been detected as a byproduct in the cell exhausts, while traces of carbonate are often found. Discriminating between carbonate formation due to real 12 e^- ethanol oxidation or atmospheric CO_2 fixation is a hard task, especially when the half cell or the DAFC anode do not operate under a protected atmosphere or at pH values lower than 13 (see below).

The chemoselectivity of ethanol electrooxidation on Pd has been recently investigated by *in situ* FTIR spectroelectrochemistry using a smooth Pd electrode at different pH values.[103] Prior to the spectroelectrochemical study, the effect of the pH on the ethanol electrooxidation was investigated by CV on 1.0 mol dm^{-3} ethanol solutions with different NaOH concentrations but similar ionic strength. The oxidation kinetics were found to depend dramatically on the pH: a peak current density was observed at pH 14, while the activity decreased for NaOH concentrations lower or higher than 1.0 mol dm^{-3}. Already at pH 12, the activity was extremely low. A similar trend has also been observed for nanostructured Pd-based electrocatalysts.[76a] An elevated concentration of OH^- groups is important to promote the oxidation reaction on Pd, yet when the concentration is too high, the hydroxyl coverage of the catalyst surface may disfavor the substrate adsorption (*vide infra*). Next to the CV study, the oxidation of ethanol on Pd was investigated by FTIR spectroelectrochemistry. A series of *in situ* FTIR spectra were acquired under potential step polarization in 1.0 mol dm^{-3} ethanol solutions at different NaOH concentrations. At NaOH concentrations ≥ 0.5 mol dm^{-3}, the characteristic bands of the acetate ion (1558 cm^{-1} and 1415 cm^{-1}) were clearly observed with no trace of either CO_2 or carbonate (Figure 33a for a 2.0 mol dm^{-3} NaOH solution). CO_2 was detected in the thin layer solution at pH values lower than 13.3, as shown by the appearance of a band at 2343 cm^{-1} whose intensity increased by decreasing the pH. Figure 33b shows the series of spectra acquired at pH 12.

A carbonate ion band (1370 cm^{-1}) was not clearly visible in these spectra due to its overlapping with the acetate band at 1415 cm^{-1}, yet its presence was inferred from the extensive broadening of the latter band. Parallel to the increase of the CO_2 band with decreasing pH, the acetate bands decreased in intensity until there was no acetate band during the forward potential step at 0.05 mol dm^{-3} NaOH. The acetate band disappeared even in the reverse potential step in 0.01 mol dm^{-3} NaOH (Figure 33b). No trace of CO was detected even at the lowest NaOH concentration investigated.

Taken altogether, these results show that the oxidative C−C bond cleavage of ethanol on Pd occurs only at NaOH concentrations lower than 0.5 mol dm^{-3} and also suggest that the oxidation of ethanol to CO_2 on Pd in moderate alkaline media proceeds either with no intermediacy of CO_{ads} (collapse of the oxidized molecule directly to CO_2) or by fast oxidation of weakly adsorbed CO by the abundant OH^-_{ads} species. The latter eventuality is less likely in view of a specific study of CO electrooxidation on Pt and Pd recently reported.[54] On the other hand, other authors have reported that the IR detection of CO_{ads} in an alkaline electrolyte is difficult even for methanol oxidation on Pt.[104] In particular, the failure to observe significant CO coverage using FTIR may be accounted for by the low steady-state CO coverage. In fact, in a solution of 0.1 mol dm^{-3} methanol and 0.1 mol dm^{-3} NaOH, the steady-state CO coverage is around 0.28 ML,[105] as compared to around 0.4 ML in a solution of 0.1 mol dm^{-3} methanol and 0.1 mol dm^{-3} H_2SO_4.[106] It is also possible that the IR detection of

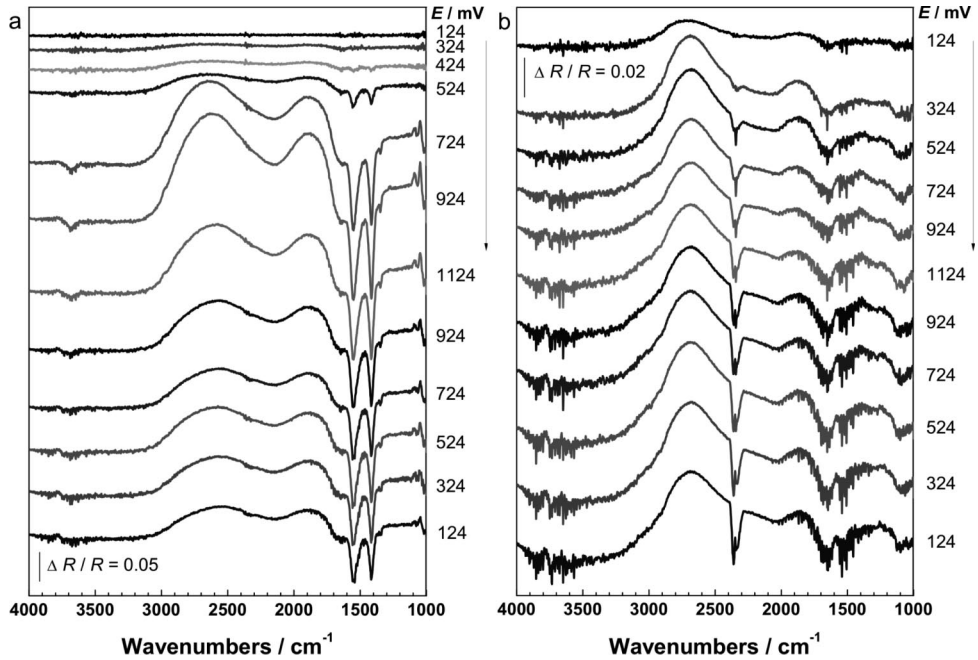

Figure 33. *In situ* FTIR spectra obtained under potential step polarization in 1.0 mol dm^{-3} ethanol with different NaOH concentrations of (a) 2.0 mol dm^{-3} NaOH and (b) 0.01 mol dm^{-3} NaOH + 0.99 mol dm^{-3} $NaClO_4$ (pH = 12). E_r = 24 mV; scan numbers, 128. Arrows indicate the potential polarization direction.[103]

CO is made particularly difficult by its low concentration, as the acetate is always the largely major product.

The mechanism of ethanol oxidation on a Pd disk electrode has been recently investigated by Zhao et al. by CV.[107] The CV studies suggest that the rate determining step is the removal of the adsorbed acyl by the adsorbed hydroxyl, while the dissociative adsorption of ethanol proceeds quickly (eqs 8−10).

$$Pd + OH^- \rightarrow Pd\text{-}OH_{ads} + e^- \quad (8)$$

$$Pd\text{-}(CH_3CH_2OH)_{ads} + 3OH^- \rightarrow Pd\text{-}(COCH_3)_{ads} + 3H_2O + 3e^- \quad (9)$$

$$Pd\text{-}(COCH_3)_{ads} + Pd\text{-}OH_{ads} \rightarrow Pd\text{-}CH_3COOH + Pd \quad \text{rds} \quad (10)$$

This study has also confirmed that a subtle balance of the EtOH and OH^- concentrations is required for high oxidation activity because the neat prevalence of either species on the catalyst surface may hinder the necessary adsorption of both species. In the same paper, it is also suggested that acetaldehyde is an active intermediate along the oxidation of ethanol on Pd, but its oxidation peak was not seen in any CV scan.

A rationale for the activity of Pd-based electrocatalysts for ethanol oxidation exclusively in alkaline media has been recently proposed.[108] DFT calculations on model Pd clusters have shown that, unlike in alkaline media, the dehydrogenation of ethanol is difficult in acidic media due to the scarcity of adsorbed hydroxyl species on the Pd surface. Figure 34 shows the potential energy profile of the initial reaction processes of ethanol oxidation on model Pd_5 and Pd_9 clusters in alkaline solution. The whole process includes two single reactions. First, the α-H atom of ethanol is cleaved and then combines with the OH^- group chemically adsorbed on Pd to give H_2O, one electron, and a CH_3CHOH_{ads}

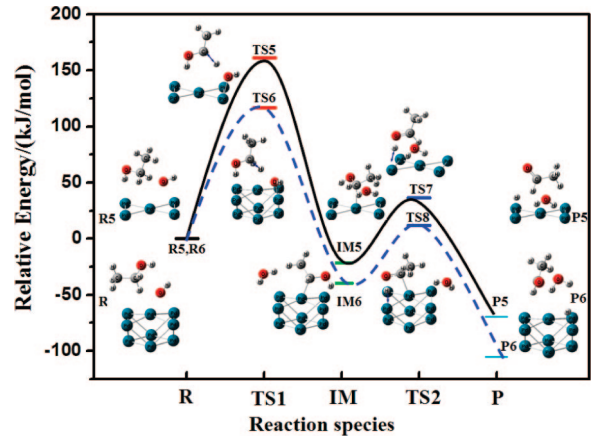

Figure 34. Potential energy profile of the initial reaction processes of ethanol oxidation on Pd_5 and Pd_9 in alkaline solution. Blue, gray, red, and white spheres represent the Pd, carbon, oxygen, and hydrogen atoms, respectively. The blue arrows represent the vibration mode at the imaginary frequency in the transition state.[108]

intermediate. TS5 and TS6 in Figure 34 represent the energy barriers of the transition states on the Pd_5 and Pd_9 clusters for this process. Subsequently, the dehydrogenation keeps going catalytically through the extraction of the hydroxyl hydrogen atom of CH_3CHOH_{ads}, leading to the formation of acetaldehyde. In this process, the transition states are TS7 and TS8 for the Pd_5 and Pd_9 clusters, respectively. The oxidation process of ethanol (eqs 11−13) is therefore similar to that reported by Homma[109,110] and Cui[111] for the hypophosphite oxidation catalyzed by nickel atoms.

$$CH_3CH_2OH + OH^- \rightarrow CH_3CHOH^- + H_2O \quad (11)$$

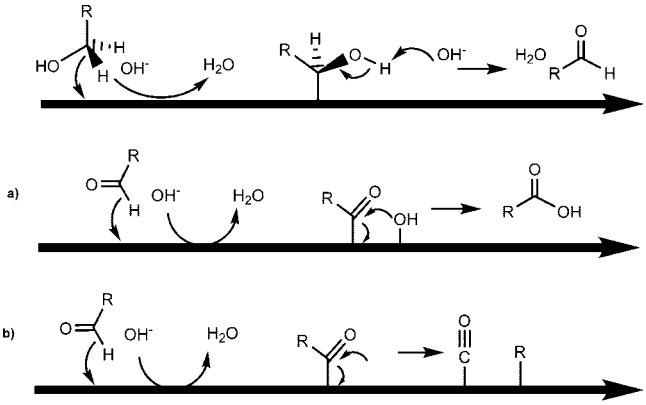

Figure 35. First steps of alcohol oxidation on metal electrocatalysts: (path a) selective conversion of alcohols into carboxylic acids; (path b) C−C bond cleavage path.

$$CH_3CHOH^- \rightarrow {}^{\bullet}CH_3CHOH + e^- \quad (12)$$

$$CH_3CHOH \rightarrow CH_3CHO + H^{\bullet} \quad (13)$$

The highest energy barriers are 116.9 kJ mol^{-1} (TS6) for the Pd_9 cluster and 161.0 kJ mol^{-1} (TS5) for the Pd_5 cluster; afterward the reaction proceeds smoothly. Both the α-H atom and the H atom on the hydroxyl group of C_2H_5OH take part in the ethanol oxidation on Pd in the presence of OH^-_{ads}. Since the energy barrier is lower on the Pd_9 cluster than that on the Pd_5 cluster in both acidic and alkaline solution, it has been suggested that the second layer of Pd atoms has a promoting action on the catalytic oxidation of ethanol.

Finally, it is worth noting that the combination of Pd nanoparticles with either metal oxides (NiO, CeO_2, Co_3O_4, Mn_3O_4)[25,52,53] or nickel−zinc alloys[58] increases both the activity and stability of the corresponding electrocatalysts for alcohol oxidation in alkaline media (*vide supra*). The beneficial effect of the added metal oxide or non-noble metal phase has been assimilated to that of Ru in Pt-Ru/C catalysts, leading to the well-known "bifunctional mechanism".[90] Within this context, metal oxides and non-noble metals would increase the concentration of OH_{ads} species on the catalyst surface, favoring the transformation of the aldehyde into the corresponding carboxylic acid via $acyl_{ads}-OH_{ads}$ coupling (path a) with respect to C−C bond cleavage to give CO_{ads} (path b) (Figure 35).

4.2. Methanol Oxidation on Pd-Based Electrocatalysts

The methanol oxidation reaction in alkaline media on Pt-based anodes has been extensively investigated over the last ten years, and an exhaustive review has been recently published.[9] In contrast, no study has appeared so far on Pd-based electrocatalysts. In view of the studies on Pt-based electrocatalysts, it is reasonable to think that also on Pd the oxidation of methanol proceeds by the intermediacy of either formate or CO (Figure 36).

Prior to CO_{ads} formation, the following adsorbates, not necessarily all of them or in sequence, have been spectroscopically detected along with the oxidation of methanol on Pt in acidic media: CH_xOH_{ads}, $-COH_{ads}$, $-HCO_{ads}$, $-COOH_{ads}$, and $(HCOOH)_{2ads}$.[112−114] A similar scenario has been validated for Pt catalysts in alkaline media, with various products depending on the potential range in which the methanol oxidation reaction has been investigated.[9] Figure

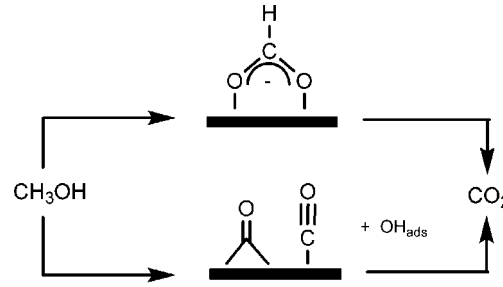

Figure 36. Reaction paths of methanol oxidation on Pt-based electrocatalysts.

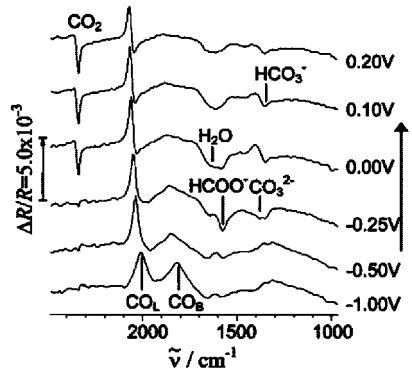

Figure 37. Curves of *in situ* rapid-scan time-resolved microscope FTIR spectra of methanol oxidation on a nanostructured Pt electrode in 0.1 mol dm^{-3} CH_3OH + 0.1 mol dm^{-3} NaOH solution with a sweep rate = 200 mV s^{-1}. Image is from ref 115.

37 shows typical curves of rapid-scan time-resolved microscope FTIR spectra of methanol oxidation on a nanostructured Pt electrode.[115]

As for Pd-based electrocatalysts in alkaline media, only *ex-situ* analytical studies of the products in the anode compartment have been reported (see section 3.2.1). In particular, both formate and carbonate have been detected, with the former transformed with time into the latter.[41]

4.3. Polyalcohol Oxidation on Pd-Based Electrocatalysts

The oxidation of EG or glycerol is more complex than that of ethanol, in accord with the presence of two and three hydroxyl groups, respectively. Figure 38 illustrates the general reaction schemes proposed for the oxidation of EG and glycerol on metal electrocatalysts. Like ethanol, polyalcohols are prevalently converted to alkali metal (poly)carboxylates on Pd-based electrocatalysts in alkaline media.[25,26,41,58,71,116] However, the oxidation of EG or glycerol yields significant amounts of carbonate. Since oxalate is very slowly oxidized on Pd-based electrodes,[25,26,41,58,71,76a,116] CO_2 (C−C bond scission) is prevalently a byproduct of the oxidation of either glycolate (Figure 38a) or tartronate (Figure 38b).

According to some authors, oxalate is not a primary product of EG oxidation but it comes from further adsorption and oxidation of glycolic acid or glycolate depending on the pH (Figure 39).[27,96,116,117]

The capacity of Pd to depress C−C bond cleavage, which results in lower overpotential and longer catalyst lifetime, has been experimentally demonstrated by Coutanceau and co-workers by investigating the EG oxidation on PtPd, PtPdBi, and PtBi catalysts in alkaline media.[27] On these electrocatalysts, EG is converted into mixtures of glycolic

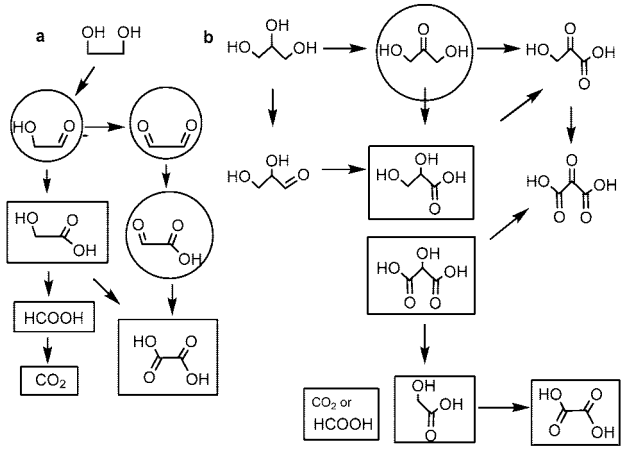

Figure 38. General schemes for EG and glycerol oxidation on metal catalysts and electrocatalysts in either acidic or basic media. Compounds in boxes have been detected in the anode compartments of DAFCs. Compounds in circles have been exclusively detected in half cells.

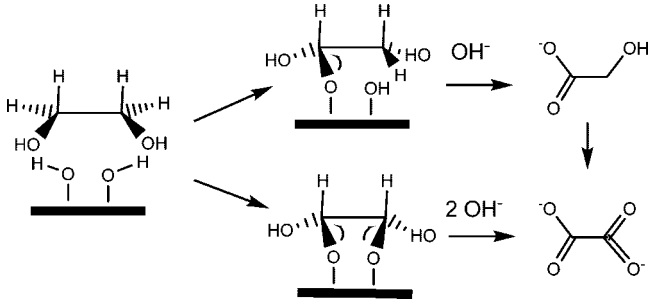

Figure 39. Proposed oxidation paths of EG to glycolate and oxalate.

acid, glyoxylic acid, oxalic acid, and formic acid, but the relative composition depends on the catalyst. It has been proposed that Bi favors the adsorption of OH species and also affects the product distribution by depressing C−C bond cleavage, like Pd.

The large numbers of possible intermediates have actually limited the effectiveness of *in situ* spectroscopic techniques, and most of the mechanistic interpretations for EG or glycerol electrooxidation rely on product analysis by IC,[97] DEMS,[96] GCMS, and ^{13}C NMR methods.[41,98]

Some IR studies are available for the EG oxidation reaction on Pt, showing CO_{ads} and CO_{2ads} species as well as several bands due to carboxylic acids such as glycolic, glyoxylic, and oxalic acid, often difficult to distinguish from each other.[97,99,116] EMIR spectroscopy has shown that the adsorption of EG at a Pt electrode is dissociative at any pH with formation of CO_{ads}.[116b] Besides confirming the presence of linearly bonded CO at high pH values, a SNIFTIR study by Christensen and Hamnett has shown the formation of glycolate, oxalate, and carbonate upon oxidation of EG on Pt in alkaline media.[116c] Based on the potential window at which these products were detected as well as the EG concentration, it was suggested that glycolate and carbonate are produced from the same intermediate (e.g., Pt-$CH(OH)CH_2OH$), while oxalate is obtained by oxidation of desorbed glycolate. Likewise, a SPAIR study of EG electrooxidation on Pt/C, PtPd/C, PtBi/C, and PtBiPd/C electrodes has provided evidence that oxalate is not a primary product of EG oxidation but it comes from adsorption and oxidation of glycolate. Traces of glyoxylic acid and formic acid were also detected by HPLC.[27] Recent studies in our laboratories have demonstrated that the electrooxidation of EG on Pd in alkaline media does not diverge substantially from that on Pt: glycolate, oxalate, and carbonate seem to

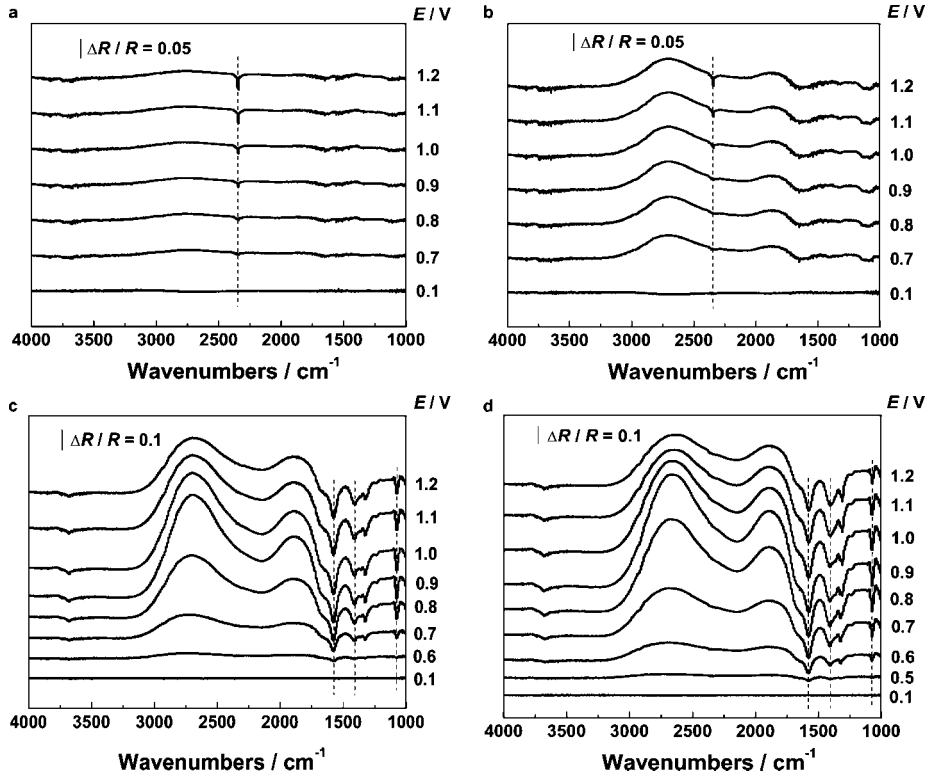

Figure 40. In situ FTIR spectra obtained under potential step polarization of the following solutions: (a) 0.01 M NaOH + 0.99 M $NaClO_4$ + 1 M EG; (b) 0.1 M NaOH + 0.9 M $NaClO_4$ + 1 M EG; (c) 1 M NaOH + 1 M EG; (d) 2 M NaOH + 1 M EG. Scan number: 128.[76a]

form at the same potential with an increase of oxalate and carbonate formation at the expense of glycolate.[76a] In particular, the electrooxidation of EG has been studied either *in situ* on a smooth Pd electrode by FTIR spectroscopy or on nanostructured Pd-based catalysts by cyclic voltammetry. Figure 40 shows some series of FTIR spectra obtained under potential step polarization on solutions of EG with different NaOH concentrations but comparable ionic strengths. At NaOH concentrations ≥ 1 M, the stretching bands of the glycolate ion at 1580 cm^{-1} (C═O) and 1070 cm^{-1} (C—O) were clearly observed together with lower-intensity bands at 1410 and 1310 cm^{-1} assignable to carbonate and oxalate, respectively (Figure 40c and d). At NaOH concentrations ≤ 1 M, the characteristic band of CO_2 at 2343 cm^{-1} was observed already at 0.7 V vs RHE. The occurrence of C—C bond breaking of an alcohol with formation of CO_2 at relatively low pH values is in line with previous reports, according to which a high OH coverage of the Pd surface is required for yielding only carboxylate products (*vide infra*).

A CV study on 2 M KOH solutions of EG has shown that the nanostructured electrocatalysts Pd-(Ni-Zn)/C, Pd-(Ni-Zn-P)/C and Pd/C are much more active than a smooth Pd electrode (up to 3300 A $g(Pd)^{-1}$) and also give different distributions of the oxidation products.[76a] Pd/C is the most selective catalyst yielding glycolate, while mixtures of glycolate (major >60%), oxalate and carbonate are obtained with Pd-(Ni-Zn)/C or Pd-(Ni-Zn-P)/C. Carbonate is produced by oxidation of both glycolate (major contribution) and oxalate, while the major part of oxalate seems to be produced by the direct oxidation of EG (Scheme 39).

No report on the electrooxidation of higher polyalcohols than EG or glycerol on Pd-based electrocatalysts has been reported so far. However, polyols such as erythritol and xylitol have been used as fuels in DAFCs with PtRu/C anodes and anion-exchange membranes,[85,118] while the D-mannose oxidation on Pt, Au and Ni electrodes in alkaline media has been uniquely investigated by CV.[100]

5. Summary

This review article describes and discusses the state-of-the art of the synthesis and characterization of Pd-based electrocatalysts for the oxidation of alcohols. It is widely documented here that Pd and Pd-alloy nanoparticles, supported on a variety of conductive materials, exhibit superior activity for the electrooxidation of alcohols and polyalcohols in alkaline solutions. Many different types of anodes containing Pd-based electrocatalysts are described which, in conjunction with anion-exchange membranes and appropriate cathodes, can be successfully employed to fabricate MEAs for monoplanar DAFCs. Fishing the best Pd-based catalyst for alcohol oxidation out of the very many examples described in this article is virtually impossible due to the different experimental conditions, in particular the Pd loading. Nevertheless, a mark of excellence can be safely attributed to the electocatalysts where Pd nanoparticles are combined with non-noble metal oxides or tungsten carbide for their excellent stability and activity at very low metal loading.

The major drawback of the known Pd-based electrocatalysts is their low propensity to cleave C—C bonds in the strongly alkaline media where they are highly active. The challenge is therefore to design new catalytic Pd architectures capable of increasing the Faradic efficiency while maintaining high electrochemical stability.

With the exception of methanol, all alcohols are prevalently oxidized on Pd to the corresponding carboxylic acids, isolated as alkali metal carboxylates. In particular, Pd-based catalysts are particularly suitable for the selective oxidation of ethanol to acetate. While this partial oxidation path represents an obstacle to the fabrication of stacks of DEFCs capable of delivering kilowatts, the good response observed at moderate temperatures in both passive and active single cells presages an effective application of Pd-based anodes to fabricate small power generators for portable electronics and first aid devices.

On the other hand, the selective oxidation of alcohols, in particular of ethanol, ethylene glycol, and glycerol to carboxylate derivatives, isolable as alkali metal salts, opens new perspectives to the use of DAFCs as reactors capable of supplying energy, with concomitant production of chemicals from renewables.[100,119−121]

6. Acknowledgments

C.B. thanks the Italian Ministry of Research (FISR project "Nanosistemi inorganici ed ibridi per lo sviluppo e l'innovazione di celle a combustibile) and the European Commission (Network of Excellence IDECAT Contract No. NMP3-CT-2005-011730) for financial support. P.K.S. acknowledges the contribution from the members of the AEMRL and the support of the Guangdong Sci. & Tech. Key Projects (2007A010700001, 2007B090400032) and Guangzhou Sci. & Tech. Key Projects (2007Z1-D0051SKT[2007]17-11).

7. References

(1) (a) Lamy, C.; Lima, A.; LeRhun, V.; Delime, F.; Coutanceau, C.; Léger, J.-M. *J. Power Sources* **2002**, *105*, 283. (b) Vigier, F.; Rousseau, S.; Coutanceau, C.; Léger, J.-M.; Lamy, C. *Top. Catal.* **2006**, *40*, 111. (c) Antolini, E. *J. Power Sources* **2007**, *170*, 1.
(2) Borup, R.; Meyers, J.; Pivovar, B.; Kim, Y. S.; Mukundan, R.; Garland, N.; Myers, D.; Wilson, M.; Garzon, F.; Wood, D.; Zelenay, P.; More, K.; Stroh, K.; Zawodzinski, T.; Boncella, J.; McGrath, J. E.; Inaba, M.; Miyatake, K.; Hori, M.; Ota, K.; Ogumi, Z.; Miyata, S.; Nishikata, A.; Siroma, Z.; Uchimoto, Y.; Yasuda, K.; Kimjima, K.-C.; Iwashita, N. *Chem. Rev.* **2007**, *107*, 3904.
(3) Cheng, X. B.; Shi, Z. A.; Glass, N. A.; Zhang, L.; Zhang, J. J.; Song, D.; Liu, Z. S.; Wang, H. J.; Shen, J. J. *Power Sources* **2007**, *165*, 739.
(4) Dillon, R.; Srinivasan, S.; Aricò, A. S.; Antonucci, V. *J. Power Sources* **2004**, *127*, 112.
(5) Membrane Technol. 2007, *November*, 8.
(6) Mauritz, K. A.; Moore, R. B. *Chem. Rev.* **2004**, *104*, 4535.
(7) Peled, E.; Livshits, V.; Duvdevani, T. *J. Power Sources* **2002**, *106*, 245.
(8) Platinum Metals Rev. 2009, *53*, 48.
(9) Spendelow, J. S.; Wieckowski, A. *Phys. Chem. Chem. Phys.* **2007**, *9*, 2654.
(10) Varcoe, J. R.; Slade, R. C. T.; Yee, E. L. H. *Chem. Commun.* **2006**, 1428.
(11) Varcoe, J. R.; Slade, R. C. T. *Electrochem. Commun.* **2006**, *8*, 839.
(12) Varcoe, J. R.; Slade, R. C. T.; Yee, E. L. H.; Poynton, D. D.; Driscoll, D. J. *J. Power Sources* **2007**, *173*, 194.
(13) Xu, T. *J. Membr. Sci.* **2005**, *263*, 1.
(14) Fang, J.; Shen, P. K. *J. Membr. Sci.* **2006**, *285*, 317.
(15) Hou, H.; Sun, G.; He, R.; Wu, Z.; Sun, B. *J. Power Sources* **2008**, *182*, 95.
(16) Scott, K.; Yu, E.; Vlachogiannopoulos, G.; Shivare, M.; Duteanu, N. *J. Power Sources* **2008**, *175*, 452.
(17) Hao, E.; Scott, K. *J. Power Sources* **2004**, *137*, 248.
(18) Xiong, Y.; Liu, Q. L.; Zhu, A. M.; Huang, S. M.; Zeng, Q. H. *J. Power Sources* **2009**, *186*, 328.
(19) Agel, E.; Bouet, J.; Fauvarque, J.-F.; Yassir, H. *Ann. Chim. Sci. Mater.* **2001**, *26*, 59.
(20) Bunawaza, H.; Yamazaki, Y. *J. Power Sources* **2008**, *182*, 48.
(21) Lu, F.; Pan, J.; Huang, A.; Zhuang, L.; Lu, J. T. *Proc. Natl. Acad. Sci. U.S.A.* **2008**, *105*, 20611.
(22) Strasser, P.; Fan, Q.; Devenney, M.; Weinberg, W. H. *J. Phys. Chem. B* **2003**, *107*, 11013.

(23) Pattabiraman, R. *Appl. Catal. A: Gen.* **1997**, *153*, 9.
(24) Zheng, H. T.; Li, Y.; Chen, S.; Shen, P. K. *J. Power Sources* **2006**, *163*, 371.
(25) Shen, P. K.; Xu, C. *Electrochem. Commun.* **2006**, *8*, 184.
(26) Coutenceau, C.; Demarconnay, L.; Lamy, C.; Léger, J. M. *J. Power Sources* **2006**, *156*, 14.
(27) Demarconnay, L.; Brimaud, S.; Coutenceau, C.; Léger, J. M. *J. Electroanal. Chem.* **2007**, *601*, 169.
(28) Huang, Y.; Zhou, X.; Liao, J.; Liu, C.; Lu, T.; Xing, W. *Electrochem. Commun.* **2008**, *10*, 621.
(29) Tian, Z. Q.; Xie, F. Y.; Shen, P. K. *J. Mater. Sci.* **2004**, *39*, 1509.
(30) Shen, P. K.; Tian, Z. Q. *Electrochim. Acta* **2004**, *49*, 3107.
(31) Zhu, L. D.; Zhao, T. S.; Xu, J. B.; Liang, Z. X. *J. Power Sources* **2009**, *187*, 80.
(32) Coloma, F.; Sepulvedaescribano, A.; Fierro, J. L. G. *Langmuir* **1994**, *10*, 750.
(33) Shao, Y. Y.; Yin, G. P.; Gao, Y. Z. *J. Power Sources* **2007**, *171*, 558.
(34) Yu, X. W.; Ye, S. Y. *J. Power Sources* **2007**, *172*, 145.
(35) Sun, Z. P.; Zhang, X. G.; Liu, R. Li.; Liang, Y. Y.; Li, H. L. *J. Power Sources* **2008**, *185*, 801.
(36) Tian, Z. Q.; Jiang, S. P.; Liang, Y. M.; Shen, P. K. *J. Phys. Chem. B* **2006**, *110*, 5343.
(37) Hu, F. P.; Shen, P. K.; Li, Y. L.; Liang, J. Y.; Wu, J.; Bao, Q. L.; Li, C. M.; Wei, Z. D. *Fuel Cells* **2008**, *8*, 429.
(38) Zhu, Z.-Z.; Wang, Z.; Li, H.-L. *J. Power Sources* **2009**, *186*, 339.
(39) Yen, C. H.; Shimizu, K.; Lin, Y.; Bailey, F.; Cheng, I. F.; Wai, C. M. *Energy Fuel* **2007**, *21*, 2268.
(40) Singh, R. N.; Anindita, A. S. *Carbon* **2009**, *47*, 271.
(41) Bambagioni, V.; Bianchini, C.; Marchionni, A.; Filippi, J.; Vizza, F.; Teddy, J.; Serp, P.; Zhiani, M. *J. Power Sources* **2009**, *190*, 241.
(42) Wang, M.; Guo, D. J.; Li, H. L. *J. Solid State Chem.* **2005**, *178*, 1996.
(43) Zhang, K. F.; Guo, D. J.; Liu, X.; Li, J.; Li, H. L.; Su, Z. X. *J. Power Sources* **2006**, *162*, 1077.
(44) Xu, M. W.; Gao, G. Y.; Zhou, W. J.; Zhang, K. F.; Li, H. L. *J. Power Sources* **2008**, *175*, 217.
(45) Xu, C. W.; Cheng, L.; Shen, P. K.; Liu, Y. L. *Electrochem. Commun.* **2007**, *9*, 997.
(46) Yuan, D. S.; Xu, C. W.; Liu, Y. L.; Tan, S.; Wang, X.; Wei, Z.; Shen, P. K. *Electrochem. Commun.* **2007**, *9*, 2473.
(47) Hu, F. P.; Wang, Z. Y.; Li, Y. L.; Liu, C. M.; Zhang, X.; Shen, P. K. *J. Power Sources* **2008**, *177*, 61.
(48) Nie, M.; Tang, H. L.; Wei, Z. D.; Jiang, S. P.; Shen, P. K. *Electrochem. Commun.* **2007**, *9*, 2375.
(49) Hu, F. P.; Shen, P. K. *J. Power Sources* **2007**, *173*, 877.
(50) Hu, X. D.; Hu, F. P.; Wang, J. G.; Shen, P. K. *Chin. J. Catal.* **2008**, *29*, 1027.
(51) Hu, F. P.; Cui, G. F.; Wei, Z. D.; Shen, P. K. *Electrochem. Commun.* **2008**, *10*, 1303.
(52) Xu, C. W.; Tian, Z. Q.; Shen, P. K.; Jiang, S. P. *Electrochim. Acta* **2008**, *53*, 2610.
(53) Xu, C. W.; Shen, P. K.; Liu, Y. *J. Power Sources* **2007**, *164*, 527.
(54) Hu, F. P.; Chen, C.; Wang, Z. Y.; Wei, G.; Shen, P. K. *Electrochim. Acta* **2006**, *52*, 1087.
(55) Lee, W.; Kim, M. G.; Choi, J.; Park, J.; Ko, S. J.; Oh, S. J.; Cheon, J. *J. Am. Chem. Soc.* **2005**, *127*, 16090.
(56) Nakashima, T.; Nohara, S.; Hiroshi, H.; Iwakura, C. *Res. Chem. Int.* **2006**, *32*, 561.
(57) Spinacé, E. V.; Neto, A. O.; Linardi, A. M. *J. Power Sources* **2004**, *128*, 121.
(58) Bambagioni, V.; Bianchini, C.; Filippi, J.; Oberhauser, W.; Marchionni, A.; Vizza, F.; Psaro, R.; Sordelli, L.; Foresti, M. L.; Innocenti, M. *ChemSusChem* **2009**, *2*, 99.
(59) Ge, J.; Xing, W.; Xue, X.; Liu, C.; Lu, T.; Liao, J. *J. Phys. Chem. C* **2007**, *111*, 17305.
(60) Bert, P.; Bianchini, C.; Emiliani, C.; Giambastiani, G.; Santiccioli, S.; Tampucci, A.; Vizza, F. *WO 009742*, 2008.
(61) Liu, B.; Li, H. Y; Zhang, X. H.; Fan, Z.; Chen, J. H. *J. Power Sources* **2009**, *186*, 62.
(62) Zheng, H. T.; Chen, S. X.; Shen, P. K. *Electrochem. Commun.* **2007**, *9*, 1563.
(63) Kumar, K. S.; Haridoss, P.; Seshadri, S. K. *Surf. Coat. Technol.* **2008**, *202*, 1764.
(64) Zhang, J.; Huang, M.; Ma, H.; Tian, F.; Pan, W.; Chen, S. *Electrochem. Commun.* **2007**, *9*, 1298.
(65) Safavi, A.; Maleki, N.; Tajabadi, F.; Farjami, E. *Electrochem. Commun.* **2007**, *9*, 1963.
(66) Xu, C. W.; Wang, H.; Shen, P. K.; Jiang, S. P. *Adv. Mater.* **2007**, *19*, 4256.
(67) Cheng, F. L.; Wang, H.; Sun, Z. H.; Ning, M. X.; Cai, Z. Q.; Zhang, M. *Electrochem. Commun.* **2008**, *10*, 798.
(68) Wang, H.; Xu, C.; Cheng, F.; Zhang, M.; Wang, S.; Jiang, S. P. *Electrochem. Commun.* **2008**, *10*, 1575.
(69) Solhy, B.; Machado, F.; Beausoleil, J.; Kihn, Y.; Gonçalves, F.; Pereira, M. F. R.; Órfão, J. J. M.; Figueiredo, J. L.; Faria, J. L.; Serp, P. *Carbon* **2008**, *46*, 1194.
(70) Carrettin, S.; McMorn, P.; Johnson, P.; Griffin, K.; Hutchings, G. J. *Chem. Commun.* **2002**, 696.
(71) Bert, P.; Bianchini, C.; Giambastiani, G.; Marchionni, A.; Tampucci, A.; Vizza, F. PCT/EP 2008/055706.
(72) Chu, D.; Wang, J.; Wang, S.; Zha, L.; He, J.; Hou, Y.; Yan, Y.; Lin, H.; Tian, Z. *Catal. Commun.* **2008**, *10*, 955.
(73) Wang, Z.; Hu, F.; Shen, P. K. *Electrochem. Commun.* **2006**, *8*, 1764.
(74) Hu, F.; Ding, F.; Song, S.; Shen, P. K. *J. Power Sources* **2006**, *163*, 415.
(75) Xu, C. W.; Tian, Z. Q.; Chen, Z. C.; Jiang, S. P. *Electrochem. Commun.* **2008**, *10*, 246.
(76) (a) Bianchini, C.; Vizza, F. Unpublished results. (b) Bianchini, C.; Bambagioni, V.; Filippi, J.; Marchionni, A.; Vizza, F.; Bert, P.; Tampucci, A. *Electrochem. Commun.* **2009**, *11*, 1077.
(77) Tarasevich, M. R.; Karichev, Z. R.; Bogdanovskaya, V. A.; Lubnin, E. N.; Kapustin, A. V. *Electrochem. Commun.* **2005**, *7*, 141.
(78) Bagchi, J.; Bhattacharya, S. K. *J. Power Sources* **2007**, *163*, 661.
(79) Wang, Z. B.; Yin, G. P.; Zhang, J.; Sun, Y. C.; Shi, P. F. *Electrochim. Acta* **2006**, *51*, 5691.
(80) htpp://www.acta-nanotech.com.
(81) Liu, J.; Ye, J.; Xu, C. W.; Jiang, S. P.; Tong, Y. *J. Power Sources* **2008**, *177*, 67.
(82) Bagchi, J.; Bhattacharya, S. K. *Trans. Met. Chem.* **2007**, *32*, 55.
(83) Verma, A.; Basu, S. *J. Power Sources* **2005**, *145*, 282.
(84) Shkolnikov, E.; Vlaskin, M.; Iljukhin, A.; Zhuk, A.; Sheindlin, A. *J. Power Sources* **2008**, *185*, 967.
(85) Matsuoka, K.; Iriyama, Y.; Abe, T.; Matsuoka, M.; Ogumi, Z. *J. Power Sources* **2005**, *150*, 27.
(86) Zhou, W. J.; Song, S. Q.; Li, W. Z.; Zhou, Z. H.; Sun, G. Q.; Xin, Q.; Douvartzides, P.; Tsiakaras, P. *J. Power Sources* **2005**, *140*, 50.
(87) Rao, V.; Hariyanto; Cremers, C.; Stimming, U. *Fuel Cells* **2007**, *7*, 417.
(88) Kua, J.; Goddard, W. A., III. *J. Am. Chem. Soc.* **1999**, *121*, 10928.
(89) Chen, Y. X.; Miki, A.; Ye, S.; Sakai, H.; Osawa, M. *J. Am. Chem. Soc.* **2003**, *125*, 3680.
(90) Yajima, T.; Wakabayashi, N.; Uchida, H.; Watanabe, M. *Chem. Commun.* **2003**, 828.
(91) Greely, J.; Mavrikakis, M. *J. Am. Chem. Soc.* **2004**, *126*, 3910.
(92) Iwasita, T.; Pastor, E. *Electrochim. Acta* **1994**, *39*, 531.
(93) Vigier, F.; Coutanceau, C.; Hahn, F.; Belgsir, E. M.; Lamy, C. *J. Electroanal. Chem.* **2004**, *563*, 81.
(94) Simões, F. C.; Dos Anjos, D. M.; Vigier, F.; Léger, J.-M.; Hahn, F.; Coutanceau, C.; Gonzalez, R. E.; Tremiliosi-Filho, C.; Andrade, A. R.; Olivi, P.; Kokoh, K. B. *J. Power Sources* **2007**, *167*, 1.
(95) Rousseau, S.; Coutanceau, C.; Lamy, C.; Léger, J. M. *J. Power Sources* **2006**, *158*, 18.
(96) Wang, H.; Jusys, Z.; Behm, R. J. *J. Electroanal. Chem.* **2006**, *595*, 23.
(97) Dailey, A.; Shin, J.; Korzeniewski, C. *Electrochim. Acta* **1998**, *44*, 1147.
(98) Gonzalez, M. J.; Hable, C. T.; Wrighton, M. S. *J. Phys. Chem. B* **1998**, *102*, 9881.
(99) Wieland, B.; Lancaster, J. P.; Hoaglund, C. S.; Holota, P.; Tornquist, W. J. *Langmuir* **1996**, *12*, 2594.
(100) Parpot, P.; Santos, P. R. B.; Bettencourt, A. P. *J. Electroanal. Chem.* **2007**, *610*, 154.
(101) Zhou, Z. Z.; Fang, X.; Li, Y. L.; Wang, Y.; Shen, P. K.; Xie, F. Y.; Zhang, X. *Electrochem. Commun.* **2008**, *11*, 290.
(102) Wei, Z. D.; Feng, Y. C.; Li, L.; Liao, M. J.; Fu, Y.; Sun, C. X.; Shao, Z. G.; Shen, P. K. *J. Power Sources* **2008**, *180*, 84.
(103) Fang, X.; Wang, L. Q.; Shen, P. K.; Cui, G. F.; Bianchini, C. Submitted for publication.
(104) Morallón, E.; Rodes, A.; Vázquez, J. L.; Pérez, J. M. *J. Electroanal. Chem.* **1995**, *391*, 149.
(105) Spendelow, J. S.; Goodpaster, J. D.; Kenis, P. J. A.; Wieckowski, A. *Langmuir* **2006**, *22*, 10457.
(106) Cao, D.; Lu, G. Q.; Wieckowski, A.; Wasileski, S. A.; Neurock, M. *J. Phys. Chem. B* **2005**, *109*, 11622.
(107) Liang, Z. X.; Zhao, T. S.; Xu, J. B.; Zhu, L. D. *Electrochim. Acta* **2009**, *54*, 2203.
(108) Cui, G. F.; Song, S. Q.; Shen, P. K.; Kowal, A.; Bianchini, C. J Phys. Chem., in press.
(109) Homma, T.; Komatsu, I.; Tamaki, A.; Nakai, H.; Osaka, T. *Electrochim. Acta* **2001**, *47*, 48.
(110) Nakai, H.; Homma, T.; Komatsu, I.; Osaka, T. *J. Phys. Chem. B* **2001**, *105*, 1701.
(111) Cui, G. F.; Liu, H.; Wu, G.; Zhao, J. W.; Song, S. Q.; Shen, P. K. *J. Phys. Chem. C* **2008**, *112*, 4601.

(112) Xia, X. H.; Iwasita, T.; Ge, F.; Vielstick, W. *Electrochim. Acta* **1996**, *41*, 711.

(113) Beden, B.; Léger, J. M.; Lamy, C. In *Modern Aspects of Electrochemistry*; Bockris, J. O. M., Ed.; Plenum Press: New York, 1992; Vol. 22, p 97.

(114) Zhu, Y.; Uchida, H.; Yajima, T.; Watanabe, M. *Langmuir* **2001**, *17*, 146.

(115) Zhou, Z. Y.; Tian, N.; Chen, Y. J.; Chen, S. P.; Sun, S. G. *J. Electroanal. Chem.* **2004**, *573*, 111.

(116) (a) Dalbay, N.; Kardigan, F. *J. Electroanal. Chem.* **1990**, *296*, 559. (b) Hahn, F.; Beden, B.; Kardigan, F.; Lamy, C. *J. Electroanal. Chem.* **1987**, *216*, 169. (c) Christensen, P. A.; Hamnett, A. *J. Electroanal. Chem.* **1989**, *260*, 347.

(117) Hauffe, W. *Heitbaum J. Electrochim. Acta* **1978**, *23*, 299.

(118) Matos, J. P. F.; Proença, L. F. A.; Lopes, M. I. S.; Fonseca, I. T. E.; Rodes, A.; Aldaz, A. *J. Electroanal. Chem.* **2007**, *609*, 42.

(119) Otsuka, K.; Ina, T.; Yamanaka, I. *Appl. Catal. A: Gen.* **2003**, *247*, 219.

(120) MeshbesherT. M. *US Patent 4,648,949*, 1987.

(121) Otsuka, K.; Yamanaka, I. *Chem. Lett.* **1988**, 753.

CR9000995